· Review · Advances in Polar Science
doi: 10.13679/j.advps.2017.4.00268 December 2017 Vol. 28 No. 4: 268-296

Spatial variability in sea-ice algal biomass: an under-ice remote sensing perspective

Emiliano CIMOLI[1*], Klaus M. MEINERS[2,3], Lars Chresten LUND-HANSEN[4,5] & Vanessa LUCIEER[1]

[1] Institute for Marine and Antarctic Studies, University of Tasmania, Hobart, Tasmania 7004, Australia;
[2] Australian Antarctic Division, Department of the Environment and Energy, Kingston, Tasmania 7050, Australia;
[3] Antarctic Climate & Ecosystems Cooperative Research Centre, University of Tasmania, Hobart, Tasmania 7004, Australia;
[4] Aquatic Biology, Department of Bioscience, Aarhus University, DK-8000 Aarhus C, Denmark;
[5] Arctic Research Centre, Aarhus University, DK-8000 Aarhus C, Denmark

Received 29 April 2017; accepted 30 December 2017

Abstract Sea-ice algae are a paramount feature of polar marine ecosystems and ice algal standing stocks are characterized by a high spatio-temporal variability. Traditional sampling techniques, e.g., ice coring, are labor intensive, spatially limited and invasive, thereby limiting our understanding of ice algal biomass variability patterns. This has consequences for quantifying ice-associated algal biomass distribution, primary production, and detecting responses to changing environmental conditions. Close-range under-ice optical remote sensing techniques have emerged as a capable alternative providing non-invasive estimates of ice algal biomass and its spatial variability. In this review we first summarize observational studies, using both classical and new methods that aim to capture biomass variability at multiple spatial scales and identify the environmental drivers. We introduce the complex multi-disciplinary nature of under-ice spectral radiation profiling techniques and discuss relevant concepts of sea-ice radiative transfer and bio-optics. In addition, we tabulate and discuss advances and limitations of different statistical approaches used to correlate biomass and under-ice light spectral composition. We also explore theoretical and technical aspects of using Unmanned Underwater Vehicles (UUV), and Hyperspectral Imaging (HI) technology in an under-ice remote sensing context. The review concludes with an outlook and way forward to combine platforms and optical sensors to quantify ice algal spatial variability and establish relationships with its environmental drivers.

Keywords **sea ice, ice algae, spatial variability, biomass, remote sensing, transmittance**

Citation: Cimoli E, Meiners K M, Lund-Hansen L C, et al. Spatial variability in sea-ice algal biomass: an under-ice remote sensing perspective. Adv Polar Sci, 2017, 28 (4): 268-296, doi:10.13679/j.advps.2017.4.00268

1 Introduction

Sea ice is a complex and dynamic three-phase medium consisting of an ice matrix permeated by brine pockets and channels, and containing air bubbles (Arrigo, 2014; Petrich and Eicken, 2009). It serves as a habitat for a variety of organisms such as viruses, bacteria, ice algae, heterotrophic protists as well as small metazoans (Arrigo, 2014; Thomas and Dieckmann, 2002). Sea ice algae assimilate carbon through photosynthesis and contribute to primary production of the polar oceans (Kohlbach et al., 2016; McMinn et al., 2007; Lizotte, 2001), influence large-scale biogeochemical cycles (Vancoppenolle et al., 2013), and determine rates of carbon export (Boetius et al., 2013). Ice algal communities form the base of the polar marine food web by providing a crucial food source for herbivore grazers during winter and spring, when pelagic food is very

* Corresponding author, E-mail: emiliano.cimoli@utas.edu.au

scarce (Kohlbach et al., 2017; Leu et al., 2015; Flores et al., 2012). Ice algae released into open waters during spring melt of the ice, can seed phytoplankton blooms (Mundy et al., 2014; Søreide et al., 2010; Smith and Nelson, 1985), with flow-on ecological effects in the underlying water column, coastal benthic zones and the deep sea (Boetius et al., 2013; Post et al., 2013; McMinn et al., 2012). In addition, ice algae can affect sea-ice physical properties due to absorption and conversion of solar energy into heat, thereby enhancing the localized melting of the ice (Castellani et al., 2017; Zeebe et al., 1996).

Sea-ice algae biomass is characterized by high spatio-temporal variability (Arrigo, 2017, 2014; Leu et al. 2015) (Figure 1). Reported depth-integrated biomass values per unit area can range from 1 to 340 mg chlorophyll-*a* (chl-*a*)·m^{-2} in the Arctic and from <1 to 1090 mg chl-*a*·m^{-2} in the Antarctic (Arrigo, 2017), however, they are typically <100 mg chl-*a*·m^{-2} and often <10 mg chl-*a*·m^{-2} in Antarctic pack ice (Meiners et al., 2012).

High ice algal horizontal patchiness has been observed across multiple spatial scales by different means (Figure 1). These include ice-coring studies using chl-*a* as a biomass proxy (Meiners et al., 2012; Gradinger, 2009) as well as fluorometric measurements of the ice-water interface *in situ* (Rysgaard et al., 2001).

At the millimeter-scale, ice algae display poorly understood distribution patterns across the skeletal ice layer (Lund-Hansen et al., 2016; Hawes et al., 2012). At the decimeter scale, chl-*a* concentrations can vary by one order of magnitude within less than one meter (Steffens et al., 2006; Spindler and Dieckmann, 1986). At the meter to kilometer scale (mesoscale), considerable variations in chl-*a* concentrations between sampling stations have been observed and linked to different sea-ice types and environmental properties such as snow cover (Meiners et al., 2017; Lange et al., 2016; Gradinger, 2009; Ryan et al., 2006a) (Figure 1).

Greater complexity of ice algal biomass variability is added if the vertical distribution (Arrigo, 2014; Meiners et al., 2012) and the temporal evolution are considered (Leu et al., 2015). Ice algal biomass is typically concentrated in the bottom-ice layers (< 0.1 m) and at the ice-water interfaces with access to nutrient-rich under-ice water (Arrigo, 2014). However, high biomass can occur in surface and internal sea-ice layers directly depending on variations in the sea-ice physical properties influenced by snow-loading, melt and flushing, infiltration from seawater, as well as ice growth processes (Arrigo, 2014; Meiners et al., 2012; Fritsen et al., 2011).

High ice algal biomass temporal variability has been observed on seasonal, monthly and weekly scales (Campbell et al., 2015; Leu et al., 2015; Lund-Hansen et al., 2014; Sibert et al., 2010). Following a typically dormant winter season, biomass growth can encompass 3−4 orders of magnitude over the course of the spring bloom. Consequently, the differentiation between temporal and spatial variability blurs for measurements taken during the spring season with inevitable consequences for the comparison of observational studies from different areas (Leu et al., 2015).

Furthermore, distinct regions and sea-ice types demonstrate different ice algal community structures and biomass ranges (Arrigo, 2014; Meiners et al., 2012). Algal species composition and biomass concentrations differ significantly between Arctic, Antarctic and non-polar ice-covered marine ecosystems (Arrigo, 2017, 2014; Kaartokallio et al. 2017; Horner et al., 1992). Differences in ice type (e.g., land-fast or pack ice) or ice age (e.g., multi-year or first-year ice) play key roles in the observed chl-*a* distributions (Lange et al., 2017a, 2015; Kattner et al., 2004).

Abiotic drivers of algal spatial variability are multiple and interrelated in various ways. Large-scale horizontal patchiness can be mostly attributed to the continually changing physical properties of the sea ice such as temperature and brine salinity, as well as nutrient and light availability. The drivers are governed by latitude, season, ice dynamic and thermodynamic growth processes, seawater salinity and meteorological conditions that change on synoptic time scales (Arrigo, 2014; Arrigo et al., 2010; Mundy et al., 2005). Also, ice-bottom roughness and sub-ice hydrography, both driving ocean-ice exchange processes, have been shown to control ice algal distribution on various scales ranging from millimeters to kilometers (Lund-Hansen et al., 2016; Sibert et al., 2010). Determining how sea ice algal biomass varies and fluctuates together with different physical and biogeochemical parameters is critical to enhancing knowledge of polar marine ecosystem function and its response to environmental changes (Leu et al., 2015; Massom and Stammerjohn, 2010).

Contrary to phytoplankton biomass and primary production which can be derived from satellite-based ocean color data, sea-ice algae cannot be monitored with above surface sensors, and conventional sea-ice biomass sampling is conducted via ice-coring (Miller et al., 2015). This results in deficits in spatial and temporal observations which are primarily attributed to the coarse nature of ice-coring surveys. Other methods used to determine ice algal biomass include diver-operated fluorometers (Rysgaard et al., 2001) or simple imagery data (such as video or still photographs) (Gutt, 1995; Ambrose et al. 2005; Katlein et al., 2015b), but are also rather limited as they are either highly demanding, logistically expensive or don't provide quantitative information.

This becomes particularly critical when considering the vast areal coverage of sea ice which affects 7% of the surface of the Earth and about 12% of the oceans. Any attempts to extrapolate point data to these vast areas are inaccurate if the investigated parameters exhibit the aforementioned variability and if the magnitude of such spatial variations is unknown. Assessing spatial variability is also critical to guide sampling efforts towards suitable scales (Swadling et al., 1997). The current lack of knowledge also impedes the formulation of quantitative relationships between ice algal patchiness and other sea ice physical parameters such as snow depth and ice thickness (Meiners et al., 2017).

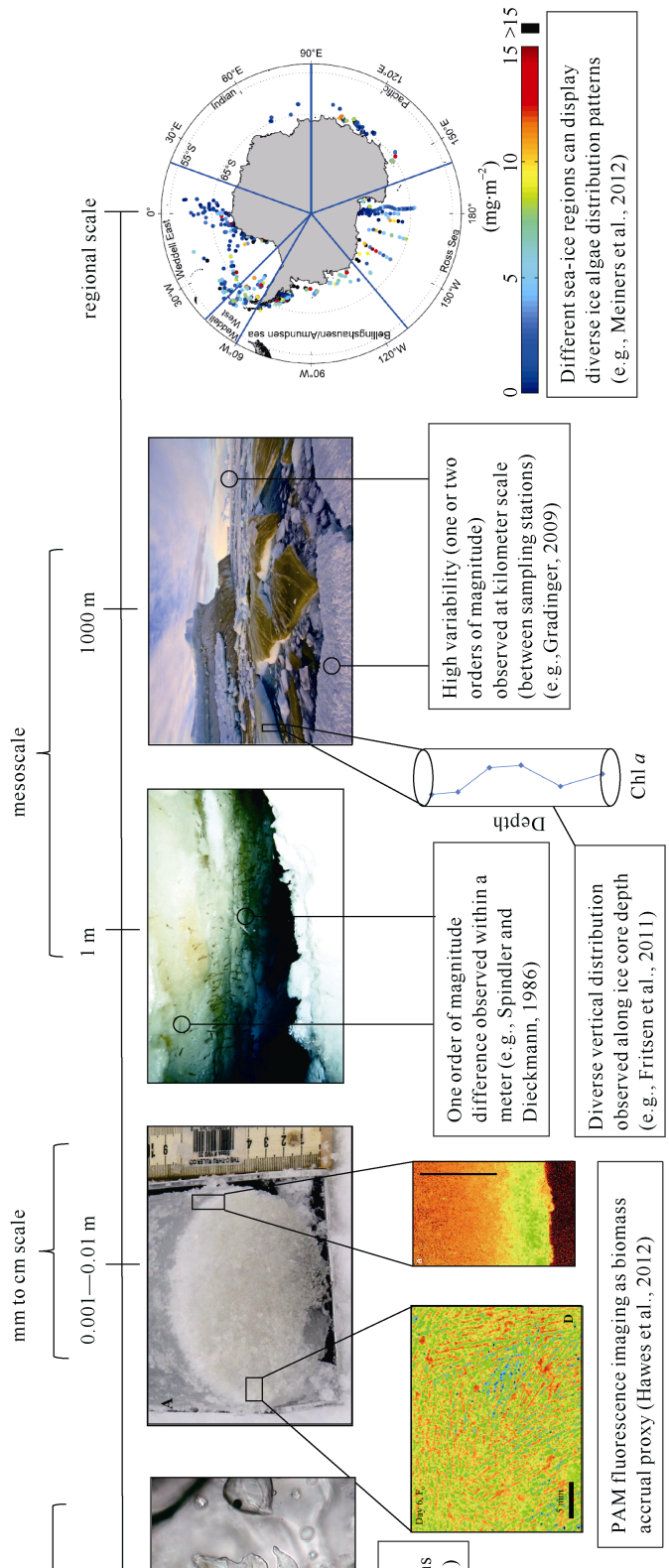

Figure 1 Overview of scles in sea-ice algae biomass spatial variability. At millimeter scale, fluorescence yield provides a good proxy of their distribution horizontally and vertically. Over the centimeter to meter scale, ice coring is the main method to estimate ice algal biomass (using chl-*a* as proxy). Vertical variability is measured by dissection of the ice cores in multiple sections providing discrete samples of the vertical distribution. Sea ice algae display diverse distribution patterns and concentration ranges across different regional sea-ice zones as well as in different ecosystems (e.g. Arctic, Antarctic and sub-Arctic areas).

Together this prevents accurate estimation of ice algal biomass and ice-associated production through up-scaling and hampers improvements in parametrization and evaluation of biogeochemical sea ice models (Steiner et al., 2016; Leu et al., 2015; Vancoppenolle et al., 2013).

In response to these sampling limitations, close-range under-ice optical remote sensing techniques are emerging as a non-invasive alternative method to quantify ice algal biomass from underneath the ice (Meiners et al., 2017; Melbourne-Thomas et al., 2015; Campbell et al., 2014; Mundy et al., 2007). Based on measured light spectra transmitted through the sea ice, empirical biomass-spectra relationships can be retrieved and used to estimate chl-*a* biomass in sea ice. An example is the identification of optimal Normalized Difference Indexes (NDIs), technique that has gained popularity due to its relative simplicity and accuracy (Wongpan et al., 2018). Once a relationship for a specific area is established, sensors can be mounted onto Unmanned Underwater Vehicles (UUVs) or ship-based under-ice trawl nets (Meiners et al., 2017; Lange et al., 2016; McDonald et al., 2015), thereby significantly improving the spatial coverage of surveys. Further advances in the methodology are in the field of Hyperspectral Imaging (HI), which has strongly improved close-range surveying approaches in other disciplines (Adão et al., 2017; Huang et al., 2014; Lu and Fei, 2014). Unlike normal radiometers, HI sensors can collect spatially continuous information from across the electromagnetic spectrum of the feature of interest, in this case, the ice-water interface. The first assessment of its application under controlled laboratory conditions has highlighted the potential of HI to provide an unprecedented view of ice algae spatial distribution through millimeter-scale resolution imagery of a square meter surface area (Cimoli et al., 2017a).

While the application of under-ice hyperspectral optical technologies *in situ* is a desirable step-forward, considerable research effort is required before its implementation as a standard field-sampling technique. Aside from understanding the complex optical properties of the target, we also need to understand the complexity associated with both dynamic under-ice sensor deployments and associated data processing techniques.

In this context, under-ice optical remote sensing methods display a highly multidisciplinary nature involving fields of marine optics, radiative transfer, photobiology and cold region engineering. Contrary to above-surface remote sensing which collects spectral data from downward looking sensors in reflection mode, upward-looking sensors under ice gather light in transmission mode. Along with optically active components within the sea-ice cover (e.g., algae, detritus, brine and air pockets, Chromophoric Dissolved Organic Matter (CDOM), and inorganic materials such as mineral particles), the light traverses an optical complex multi-phase scattering medium (the sea-ice layered matrix) and the water-column before reaching the sensor (Perovich, 1996). Therefore a series of geometric and transmissive properties of the light field need to be considered when measuring and interpreting hyperspectral data from underneath the ice (Katlein et al., 2016). Also, the layered and vertically variable sea-ice structure provides diverse microhabitats for algae with concomitant implications for their photophysiological adaptations and bio-optical properties and thus influencing spectra-biomass relationships and their inter-regional validity (Wongpan et al., 2018; Lange et al., 2016; Melbourne-Thomas et al., 2015).

Considering the growing need of observational studies capturing the highly variable sea-ice environment (Steiner et al., 2016; Miller et al., 2015; Vancoppenolle et al., 2013), the aims of this review are to provide a comprehensive overview of under-ice optical remote sensing techniques to measure algal biomass, their limitations and research prospects. This includes a discussion of the potential opportunities to improve our understanding of variability in sea-ice algal biomass, as well as the complex interactions between the associated environmental drivers.

The aims of this review can be summarized as follows:

- Review observational studies treating sea-ice algae biomass spatial variability at multiple spatial scales, and briefly schematize its environmental drivers and outline some key relationships.
- Provide a brief overview of sea-ice radiative transfer and bio-optical research relevant to sea-ice algae under-ice remote sensing methods.
- Summarize current studies employing sea-ice biomass-spectra regression algorithms derived from under-ice optical remote sensing, chart identified relationships and outline the caveats and future research fronts of the methodology.
- Explore the advances and future challenges associated with underwater camera mounting platforms such as UUVs and the implications for HI.
- Layout the research possibilities of the methodologies to improve our understanding of sea-ice algal spatial variability and identify the environmental drivers.

It should be noted that this review provides a summary of the environmental parameters that drive ice algal variability, this is not an ecological review of the sea-ice environment. The focus here is given to observational studies involving measured spatial variation of biomass at multiple spatial scales, and the efforts towards its quantification using emerging techniques. We refer to other recent comprehensive studies treating sea-ice algal phenology (Castellani et al., 2017; Leu et al., 2015) and ice-associated ecosystem function (Arrigo, 2017, 2014).

2 The drivers of sea-ice algal spatial variability

Table 1 lists relevant studies coupling biomass proxies

(such as chl-*a*) with other sea-ice environmental parameters in a spatial analysis context. We refer to spatial variability as to any variation of the biomass proxy's magnitude over space associated with changes in the sea-ice environment. It's important to notice that the magnitude of variation is typically relative to the studied site. For instance, in Kangerlussuaq (Greenland), measured biomass varies around 0.5—1 mg chl-$a \cdot m^{-2}$ (Lund-Hansen et al., 2014) and an increase by 0.5 mg chl-$a \cdot m^{-2}$ is considered very high. In contrast, at Cape Evans (Antarctica), biomass abundance has been observed to vary spatially between 4.4 and 143 mg chl-$a \cdot m^{-2}$ (Ryan et al., 2006).

Table 1 Compilation of observational studies on sea-ice algal biomass spatial variability (as chl-*a* or other proxy) and associated environmental drivers. The table follows an increasing order of spatial sampling scale and resolution. FYI refers to First Year Ice, MYI to Multi-Year Ice. PAM refers to Pulse Amplitude Modulated (fluorometry). Statistical method used refers to the method employed (if any) to assess spatial variability or to estimate the correlations between biomass proxies and any of the analysed co-variates. ANOVA stands for analysis of variance

Study	Region/Ice type/Date	Methods	Biomass variability scale observed	Main biomass variability drivers assessed and statistical method employed (if any)
Hawes et al., 2012 Lund-Hansen et al., 2014 Lund-Hansen et al., 2016	• Kangerlussuaq, West Greenland • FYI in a frozen fjord • March—April 2011	Ice coring and PAM fluorescence imaging	Daily time series of sub-millimeter resolution PAM imagery (30 × 23 mm^2). Visualization of brine channels, ice crystals and mm-scale distribution and accrual.	Brine channel evolution, ice crystal development, and salinity. Snow-cover (through artificial removal) and photophysiology. Ice growth, surface roughness, water flow and nutrient availability. Inquires role of ice-water boundary layer and ice roughness.
Krembs et al., 2002	• Experimental ice tanks with water flows and observable structure relief	Ice tank samples and visual inspection	cm scale variability observed along specific sections of experimental ice tank.	Under-ice relief structure. Water flow altering pore water flux regimes and influencing nutrients exchange.
Rysgaard et al., 2001	• Young Sound, Northeast Greenland • FYI and MYI. • June—July 1999	Ice coring and diving PAM	Incremental cm scale samples over L-shape 10 m transects. Process repeated for multiple sampling stations (100 $s \cdot m^{-1}$). High variability on 50—100 m patches. Low variability on 0.025—5 m patches.	Light availability, algae photosynthetic activity, influence of grazing and physical removal/inhibition of algae by salinity fluctuations. Differences in pack ice and fast ice. Employs spatial autocorrelation to analyse the 2-dimensional distribution.
Eicken et al., 1991	• North-western Weddell Sea • MYI (2 years) ice floes • October—November 1988 and September— October 1989	Ice coring	Grids of gradual spacing (0.25 m, 2 m, and 20 m). Process repeated at mesoscale (km) distance on different floes. Variations up to one order of magnitude on < 2 m. Variability found almost independent of scale.	Ice texture, salinity, pore structure, and nutrient concentrations. Differences in second-year ice and first-year ice.
Swadling et al., 1997	• Davis Station, East Antarctica • Fast Ice • April 1994	Ice coring	Hierarchical sampling at the mesoscale (m to km). High variability between locations at the km scale and high patchiness at 0.5—1 m apart.	Salinity, chl-*b*, and metazoan abundance. Employs 3-factor nested analysis of variance (ANOVA) to assess variation.
Ambrose et al., 2005	• Chukchi Sea • FYI • June 1998	ROV algal cover imagery and ice coring	Mesoscale transects of 20—85 m for different stations which are tenths of km apart. 1 m deployment depth. 1 cm resolution of the images.	Snow depth, ice thickness, ice structure, ice salinity, water pigments. Algae cover correlation with floe edge distance. Discuss transport over benthic systems. Employs Pearson correlation coefficients to examine relationships.

Continued

Study	Region/Ice type/Date	Methods	Biomass variability scale observed	Main biomass variability drivers assessed and statistical method employed (if any)
Gosselin et al., 1986	• Southeastern Hudson Bay and Manitounuk Sound (Subpolar estuarine) • FYI • May 1982	Ice coring	Hierarchical sampling over horizontal transects. Large (30 km) and small (0.3 to 500 m) spatial scales analyzed.	Snow depth, ice thickness, light availability and salinity (or pore space). Infers role of wind over snow drifting and re-distribution influencing light availability. Used spatial autocorrelation to analyse 2-dimensional distribution of the variables.
Monti et al., 1996	• Southeastern Hudson Bay. • FYI • April—May 1989—90	Submersible ice coring	Sampling at five stations at 5 km distance between each other.	Salinity, nutrients, diversification of algal species and ice-water interface properties (currents). Relationships quantified using canonical correspondence analysis.
Welch and Bergmann, 1989	• Resolute, N.W-T, Canada • FYI (congelation ice) • 1984—86	Ice coring	Long-term study of variability controls over different sampling stations at tenths of km distance.	Grazer's abundance, light availability, nutrients and habitable pore space. Differences in old and new ice.
Arrigo et al., 2014	• Amundsen Sea. • Diverse ice types. • December 2010—January 2011	Ice coring	Zonal transect surveys at multiple sampling stations distanced hundreds of km.	Nutrients, salinity, temperature, ice thickness, snow depth, optical properties (including pigment composition) and surface flooding.
Gutt, 1995	• Northeast Greenland • FYI • June 1993	ROV imagery descriptive analysis	One 150 m transect.	Under-ice topography linked with different types of under-ice algal aggregations.
Fritsen et al., 2011	• Bellingshausen Sea • FYI • September 2007	Ice coring	Different vertical distributions of chl-*a* within three sites 50—75 m distant.	Snow cover, ice thickness and optical properties on vertical variability.
Lange et al., 2015	• Lincoln Sea • FYI and MYI. • Three consecutive spring seasons from 2010 and 2012	Ice coring	m distance samples for various stations at km scale distance.	Snow depth, ice thickness, ice texture, salinity and presence of hummock features. ANOVA for effect of ice age classes and texture. Logistic regression for influence of snow depth and derived optical properties.
Li et al., 2016	• Weddell Sea • Different types of sea ice • August—October 2006	Ice coring	Samples at several stations separated by km distance and mainly looks at vertical distribution.	Ice core texture, porosity, ice thickness, temperature, salinity and pigment content.
Spindler and Dieckmann, 1986	• Weddell Sea • January—February 1985 • One fast ice station and one Ice floe	Ice coring	Parallel sampling at 30 cm apart and transects of 3 km separated. Observed high variability at 30 cm apart meanwhile at 3 km distances did not observe high variability.	Foramiferal abundances and salinity.
Steffens et al., 2006	• Gulf of Bothnia, Baltic Sea • Different types of ice • March 2004	Ice coring	Hierarchical sampling with spacings of 10 cm, 2.5 m, 25 m, 250 m and 2.5 km. Observed high variability for all the spatial scales.	Ice salinity, pheophytin content, dissolved nitrate plus nitrite, dissolved organic carbon and nitrogen, snow depth, ice thickness and ice structure. Parameters analysed with nested ANOVA. Pairwise relationships using Spearman correlation. Multivariate relationships using principal component analysis.

Continued

Study	Region/Ice type/Date	Methods	Biomass variability scale observed	Main biomass variability drivers assessed and statistical method employed (if any)
Meiners et al., 2017	• Weddell Sea • Pack ice floe • September 2017	ROV based under-ice optical remote sensing	100 m by 100 m area. Effective grid resolution of 1 m. Observed within floe scale patchiness of sea ice algae.	Snow depth, ice thickness and sea ice freeboard. Empirical variograms to explore scales of spatial variability. Relationships analysed with Generalized Additive Model approach.
Granskog et al., 2005	• Gulf of Finland, Baltic Sea • FYI, Landfast ice • February, March and April 2003	Ice coring	Mesoscale transects from 40 km to small <20 m scales. At small scales samples in arrays with core spacing of 0.2 m, 2 m, and 20 m. No evidence patchiness at scales <20 m. Sampled over ice season for small-scale patchiness.	Salinity (ice porosity), stable oxygen isotopes, nutrients and dissolved organic carbon. Relationships between parameters studied using non-parametric Spearman rank-order correlation.
Robineau et al., 1997	• Saroma-ko Lagoon, Sea of Okhotsk • March 1992	Ice coring	Three scales of variation were considered. From the mesoscale (0.02—4 km) to small horizontal variability (0.2—10 m).	Snow depth, ice thickness and ice-bottom salinity. Assessment using linear correlations complemented by path analysis.
Lange et al., 2016	• Central Arctic Ocean • Different ice types from ponded ice, snow and ponds frozen, no snow and ponds, frozen surface (FYI, MYI) • August—October 2011	ROV and SUIT based under-ice optical remote sensing	Various transects from 30 to 210 m for the ROV. Two transects of 800 and 1500 m respectively with under-ice trawl system. Finds high variability at the mesoscale.	Focus on regression model performance.
Garrison and Kurt, 1991	• Weddell Sea /Scotia Sea • Pack ice both FYI and MYI floes • Austral Spring 1983	Ice coring	Multiple sampling stations at km distance. Investigates vertical variability, mainly surface layer assemblages. Higher biomass at the edge of the floes.	Snow depth, floe thickness, floe size, salinity and other chemical measurements/nutrients. Infers on grazing influence. Correlation analysis among parameters.
Fiala et al., 2006	• Pointe Géologie Archipelago, Terre Adelie • Land-fast FYI • April to December 1998	Ice coring	Multiple seasonal and spatial samples at different stations at km scale distance. Investigates vertical variability and surface assemblages.	Nutrients and ice formation and inclusion of available phytoplankton in underlying water column.
Lange et al., 2017a	• Lincoln Sea • MYI and FYI sites including land-fast and pack ice • May 2010, 2011 and 2012	Ice coring	A set of three ice cores for a total of 18 different sites at km distance.	Ice types, differences in MYI-Hummock ice and FYI. ANOVA was performed to investigate correlations.
Meiners et al., 2012	• Antarctic circum-polar study • 25 years of data	Ice coring	Data compilation analysing vertical variability over several regions in Antarctica.	Ice thickness, vertical distribution and regional characteristics.

For each study, Table 1 includes location, ice type, date of the survey, sampling method employed, spatial scale examined, main environmental parameters measured or discussed and the spatial analysis method applied (if any). Rows of Table 1 follow an increase of spatial sampling scale. The table emphasizes the high spatial variability observed at all the scales ranging from the millimeter to the mesoscale for both polar regions as well as temperate ice-covered areas.

The most common proxy employed for mapping ice-algae distribution is chl-*a* concentration measured on melted sea-ice samples obtained by coring (Miller et al., 2015). However, other techniques such as the fluorescence-based Diving-PAM (Pulse Amplitude Modulated fluorometry) (McMinn and Hegseth, 2007), the Imaging-PAM (Hawes et al., 2012) and standard RGB imagery (Katlein et al., 2015b; Gutt, 1995) have also been applied. At this stage, only a few studies employ under-ice light spectra to biomass conversion algorithms to monitor spatial variability. A limited number of emerging numerical models feature tests on drivers of biomass variability on large-scales (Castellani et al., 2017; Tedesco and Vichi, 2014; Sibert et al., 2010), though numerical models are out of the scope of the review, and will not be considered further.

Table 1 gives qualitative insights into the main drivers of ice-algal variability, the survey locations and ice types and highlights the diversity among studies ranging from FYI and MYI to pack and fast ice. The observed spatial scales and seasons vary significantly across the tabulated investigations which are scattered from years 1982 to 2018. Consequently, a clear differentiation between inter-annual, seasonal and the multiple scales of spatial variability remains problematic. Also, some studies only sample the bottom of the ice core, while others have integrated chl-*a* over the entire ice thickness, raising questions on the studies comparability and potential biases in the auxiliary parameters (Meiners et al., 2012).

Here we differentiate drivers of ice-algal biomass spatial variability between sea-ice physical properties and the properties of the ice algae biological medium. While the first refers to sea-ice physical properties that can be measured in units of distance and space, the latter refers to properties of the medium (e.g., sea brine) which immediately surrounds the organisms.

Sea-ice physical properties and properties of the ice algae medium are highly inter-correlated and are driven by continually varying temperature gradients at the ice-atmosphere interface (e.g., influenced by wind and precipitation) and at the ice-water interface (e.g., influenced by the properties of the underlying water column and overall hydrographic regime) (Meiners and Michel, 2017). Figure 2 provides a schematic of this complex and closely coupled system. The physical properties of sea-ice include snow depth, ice thickness, under-ice topography, surface conditions and ice structure (including porosity, brine/gas volumes, and ice crystal type). The properties of the ice algae medium include nutrient concentrations, salinity and temperature among others. While the sea ice physical properties govern the light distribution and habitat conditions for ice algae, the medium properties, together with light, govern growth and physiological activity of the organisms.

Overall, sea-ice physical properties and ice algae medium properties are strongly dependent on the particular geographic region as well as the time of the year (Fritsen et al., 2011; Steffens et al., 2006; Rysgaard et al., 2001; Gosselin et al., 1986). From Table 1, depending on the spatial scale and the time of the year considered, the primary drivers promoting ice algal spatial variability can differ and are briefly presented in the next section.

2.1 Sea ice formation, decay and age

Sea-ice physical processes play a significant role in the vertical and horizontal distribution of sea-ice algal biomass (Arrigo, 2014; Meiners et al., 2012). They shape available space for the sea ice algae to inhabit and determine whether algal communities thrive at the bottom of the sea-ice cover, within the internal brine channel system or in surface layers (Arrigo, 2014). The initial inputs of algae to the sea-ice system occurs during the inclusion of biological material during ice formation and thereafter through accrual at the deformed ice sub-surface (Figure 2) (Janssens et al., 2016; Lund-Hansen et al., 2016; Lange et al., 2015; Arrigo, 2014). Algal growth rates and accumulation from the underlying water column are controlled by the interplay of sea-ice physical properties and medium conditions. Biomass loss can be attributed to brine loss (flushing) from increased permeability, ablation at the ice underside (Li et al., 2016) and release into open waters during ice melt (Leu et al., 2015; Arrigo, 2014). Grazing losses may also occur, but grazing on ice algae by heterotrophs remains poorly quantified (Bluhm et al., 2017; Meiners and Michel, 2017).

Depending on the surface ocean conditions, which can be either being calm or turbulent, sea ice can form as congelation or frazil ice, respectively (Arrigo, 2014; Petrich and Eicken, 2009). In calm conditions, and once an initial ice cover has been established, congelation ice formation takes place as vertically parallel ice crystals forming a continuous sheet that propagates downward. The propagation margin is referred as the skeletal layer and gives origin to the sea ice columnar/lamellar structure (Petrich and Eicken, 2009). This type of ice is a common feature for coastal fast ice. Frazil ice is instead associated with turbulent conditions (more typical of open ocean conditions) and induces ice crystals to consolidate first into grease ice and later into pancake ice. Pancake ice is then merged to form a consolidated sheet which can then initiate vertical ice growth (e.g., with a skeletal layer margin at the bottom) (Arrigo, 2014; Petrich and Eicken, 2009). Frazil ice formation is more typical for open ocean conditions, and when sea ice is free-drifting, it is referred to as pack ice.

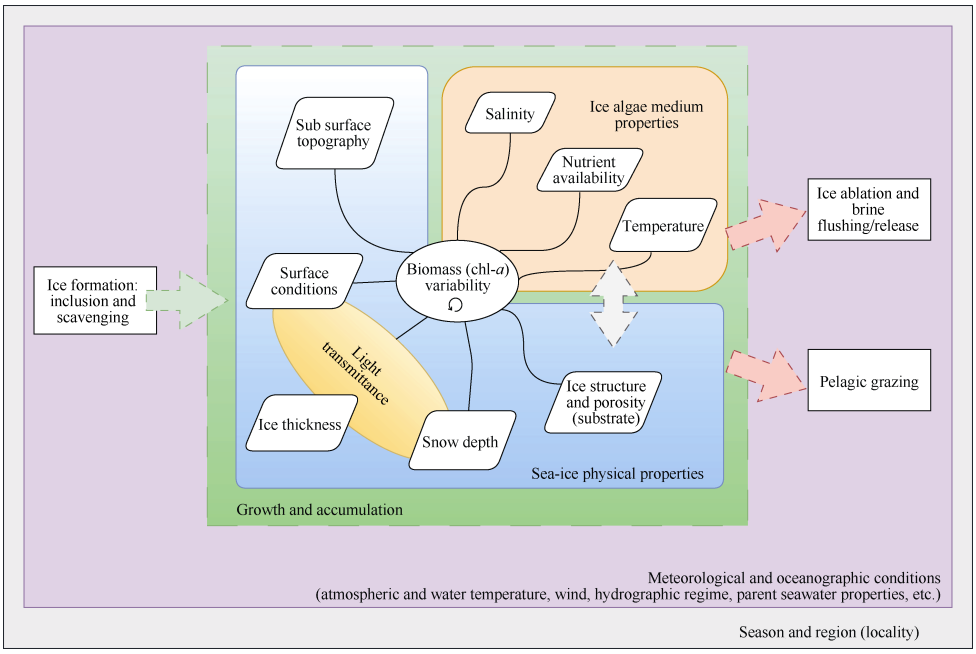

Figure 2 Simplified schematic of drivers influencing the spatial distribution of biomass in sea ice. Green arrows imply the initial biomass input to the system and red arrows the system output. The grey arrow symbolizes the close correlation between sea-ice physical properties and the properties of the ice algae medium. Some sea-ice physical properties are also closely correlated with each other. Overall, all parameters are heavily influenced by temperature and by the meteorological and oceanographic conditions which in turn are dependent on the location and season of the year.

High spatial variability of biomass has been observed for both land-fast and pack ice (Table 1), with similar factors influencing settlement and accumulation of algae in both ice types. However, there are fundamental differences between pack ice and land-fast ice formation (Gradinger and Ikävalko, 1998; Spindler, 1994). In the early stages of ice formation, the open ocean setting of pack ice is associated with the scavenging of suspended biological material by raising frazil crystals and higher initial seawater and salt content in the pre-dominant frazil ice type compared to newly formed congelation ice (Arrigo, 2014; Spindler, 1994). This facilitates the consequent development of so-called internal communities which are a common feature in Antarctic pack ice (Meiners et al., 2017; Arrigo, 2014). Internal communities are also associated with ridging and rafting of ice floes, as well as with melting and refreezing processes of multi-year sea ice (Welch and Bergmann, 1989). Pressure ridges, for example, can incorporate water pockets during formation, which are suspected to represent a nutrient reservoir for algae (Spindler, 1994).

An additional type of ice originates from flooding and refreezing of seawater that has infiltrated into the overlying snow layer. Flooding can happen either via snow loading of sea ice or through deformation of ice floes. Seawater at the ice surface forms slush ice and snow ice if it refreezes (Arrigo, 2014; Petrich and Eicken, 2009). Surface flooding and the snow-ice formation are characteristic of Antarctic pack ice but have also been reported for other ice types (Petrich and Eicken, 2016). In the Antarctic pack-ice zone, mesoscale differences in these physical processes are often the main factors that drive the high biomass variability (both on horizontal and vertical dimensions) as a result from flooding and increased supply of nutrients and biological material (Meiners et al., 2017, 2012; Fritsen et al., 2011; Garrison and Kurt, 1991).

The influence of ice age on biomass still requires further research efforts. Some Arctic studies report no significant differences between FYI and MYI (Lange et al., 2015), while others suggest that repeated melting and re-freezing cycles favour ice algal accumulation, build up and inclusion in MYI (Granskog et al., 2005; Eicken et al., 1991; Welch and Bergmann, 1989). For Antarctica, Fiala et al. (2006) reported high biomass in FYI fast ice when compared to pack ice. Meiners et al. (2011) hypothesized that persistence of sea-ice into the late spring/early summer might increase biomass build-up in East Antarctic first-year pack ice. The role of ice age is also suspected to play a role in the seeding and distribution of algal populations in a phenomenon referred as the “multiyear ice seed repository hypothesis” (Olsen et al., 2017). The hypothesis suggests that cells trapped in surface layers of ice that survives a summer season function as a seed repository. They are released as temperatures increase in the spring season and seed the ice algal spring bloom in sea-ice bottom layers and adjacent ice floes.

2.2 Sea-ice structure, temperature, nutrients and salinity

Sea-ice is characterized by strong time-varying vertical gradients in temperature, brine salinity, pore space, and permeability that continuously shape the habitability of the sea-ice environment (Arrigo, 2014; Vancoppenolle et al., 2013; Petrich and Eicken, 2009). These gradients, together with other sea ice physical processes mentioned above, control nutrient availability and brine salinity in the interstitial channel system in which the ice algae thrive, and play an important role in the small-scale vertical distribution of algae communities within the ice (e.g., bottom, internal or surface) (Arrigo, 2014; Legendre and Gosselin, 1991).

Sea-ice porosity is considered as a particular index in evaluating the relationship between sea-ice physical parameters and chl-*a* because porosity comprises the ice temperature, salinity, and density (Li et al., 2016). Ice algae prefer conditions that provide ready access to nutrients in the seawater, salinity levels that do not limit growth rates, and sufficient light for photosynthetic activity (Arrigo, 2014). During spring, as a result of increasing ice temperatures, habitable pore space (porosity) at the bottom is higher than in other sea-ice layers (Tedesco and Vichi, 2014) and most of the biomass is usually found in the lowermost 0.05 – 0.1 m of the ice, due to the direct contact with sea water allowing the infiltration of nutrients and resulting in favourable brine salinities (Arrigo, 2017; Cota and Ralph, 1991). Looking at these bottom communities, microscale studies using novel PAM fluorescence imaging approaches have provided different proxies (such as minimal fluorescence yield, F_o) for evaluating changes in algal biomass over time (Lund-Hansen et al., 2016; Hawes et al., 2012). Hawes et al. (2012) highlighted how brine channel evolution and skeletal layer development triggered algae population growth. In fact, while sea ice algal cells can grow despite exposure to extremes in temperature and salinity, the high salinities found within the brine channels, reaching up to 100 or higher, can reduce growth rates of internal communities (Arrigo, 2014; Krembs et al., 2000).

The influence of sea-ice physical properties such as the ice texture, crystal type and brine volume, on sea ice biological properties, has been highlighted by Li et al. (2016), and Spindler (1994) to mention a few. The more recent study by Li et al. (2016) showed a strong statistical relationship between chl-*a* and brine volume (porosity). Quantitative relationships such as this are rare due to the great effort involved in acquiring extensive ice coring datasets. They are, however, extremely useful for augmenting our understanding ice algae variability drivers towards improved modeling results (Steiner et al., 2016). More studies are required coupling proxies of porosity, such as temperature and bulk salinity, with chl-*a* for diverse types of ice covers and over time for a better parametrization of these drivers.

Ice salinity and temperature can also vary horizontally from the sub-meter to regional scales (Eicken et al., 1991; Tucker et al., 1984). As habitable pore space co-varies with the salinity and temperature of the ice (Cox and Weeks, 1983), they also consequently influence the horizontal distribution of ice algae. It's important to consider that ice-bottom salinity (and nutrients) are not only correlated to the sea-ice structure but are also directly influenced by properties of the underlying waters. Observational studies at the mesoscale have consequentially observed biomass variability along with variations in seawater salinity (Gosselin et al., 1986), nutrients (Cota and Ralph, 1991; Maestrini et al., 1986) and under-ice currents (Monti et al., 1996).

2.3 Under-ice topography

There are very few qualitative studies and no quantitative studies treating under-ice roughness and topography as a parameter influencing ice algal biomass distribution. However, it is suspected that under-ice topography plays an influential role in shaping hydrographic regimes at the ice-water boundary layer, partially explaining the high natural variability of the sea-ice organisms. A pioneering study investigated this aspect in experimental set-ups and monitored brine channel evolution, drainage and surface roughness (topography) together with biomass (Krembs et al., 2002, 2001). The study suggested that water flow under varying under-ice topographies alters pore water flux regimes and nutrient exchange promoting differential algal biomass accumulation.

At the millimeter scale, in a PAM imaging study, biomass distribution was compared to ice growth, surface roughness, water flow, and nutrient availability among other factors in the Arctic (Lund-Hansen et al., 2016). The study identified ice roughness as the most relevant factor in the accrual of diatoms at the water-ice interface. The relative importance of advection and accrual of biomass from the underlying ocean was emphasized rather than *in situ* growth from biomass initially incorporated into the sea ice. Physical accumulation of biomass through advection remains a poorly understood aspect of ice algae bloom dynamics.

In the Arctic, at the sea-ice floe scale, the topography and hydrographic regime under the ice have been found to influence algae distribution through trapping of ice algal aggregates (Katlein et al., 2015b). During late summer ice algal aggregates accumulate in dome-shaped structures and at the edges of pressure ridges. Overall, more investigations are required to better understand processes at the water ice boundary layer regarding nutrient exchange and algal aggregation at both small and large spatial scales, and at different times of the year.

2.4 Snow, light and surface properties

Together with nutrient availability, light is the most critical

factor influencing ice algal photosynthesis and growth (Cota and Smith, 1991) and several studies have recognized light as the main limiting factor controlling bloom initiation during the winter-spring season (Leu et al., 2015; Rysgaard et al., 2001; Gosselin et al., 1986). While at small scales the ice microstructure influences algae distribution patterns (Lund-Hansen et al., 2016), boosts growth by allowing nutrients to permeate (Li et al., 2016) and fosters accrual of biologic material (Krembs et al., 2002), at the mesoscale level, ice algae patchiness is mostly associated with the spatial variability in physical sea-ice properties governing light transmittance (Palmisano, 1987; Gosselin et al., 1986) (Figure 2). Indeed light availability in a given under-ice environment is not only a function of the location (latitude) and incoming Photosynthetic Active Radiation (PAR) (Ehn and Mundy, 2013) but also of the meteorological conditions (e.g. cloud cover) (Raymond et al., 2009), sea ice surface conditions and ice thickness (Perovich, 1996). Light available for photosynthesis of sea-ice algae is mostly influenced by the snow cover (depth and age) due to its high attenuation coefficients and the high albedo rather than the ice itself (Perovich, 1996; Palmisano, 1987).

Ice thickness and related variations in ice morphology, being compounded by deformational processes, also contribute to variability in light intensities. As an example, a recent Arctic study highlighted that chl-*a* concentrations in thick MYI are unusually high due to the presence of surface hummocks which have a relatively thin overlying snowpack, thereby fostering algal accumulation due to increased light levels (Lange et al., 2017a, 2015). Surface properties such as melt-pond coverage or surface flooding due to snow loading also play a role in the amount of light available for ice algae beneath the snow and ice pack (e.g., Arndt et al., 2017; Katlein et al., 2015b). Increasingly frequent leads in Arctic sea ice are also capable of re-defining the ice structure and optical properties and have a significant impact on light transmittance and availability for under-ice communities (Kauko et al., 2017).

Although increased light intensities are typically associated with favorable growth conditions, the relationship is not straightforward in sea ice and varies depending on the season, and ice algae light exposure history. For example, while Arctic land-fast sea-ice algae biomass is inversely correlated with snow depth early in the season due to less light availability (Mundy et al., 2005; Welch and Bergmann, 1989), multiple studies have observed that higher snow depth is linked to higher biomass later in the season (Campbell et al., 2015; Melbourne-Thomas et al., 2015; Fritsen et al., 2011).

Late-season positive snow depth-biomass relationship in the Arctic have been attributed to photoacclimation and photo-inhibition due to excess of light following dark adaptation by the ice algae. Ice algae experience a significant increase in irradiance between late winter and spring. They are initially light limited by the snow cover (characterised by a negative relationship), but as snow cover is removed, biomass for shade adapted communities have been observed to decline due to increases in light transmission (inducing strong photoinhibition) (Galindo et al., 2017; Lund-Hansen et al. 2014), and due to heat fluxes triggering under-ice ablation loss (Campbell et al., 2015; Juhl and Krembs, 2010). Ablation loss can also happen as a result of lowered thermal insulation under a thin snow cover. This results in stronger desalination and increased warming of the ice and eventually flushing and ice melt at the bottom. Algal stocks then get sloughed off, a process that has been proposed in various studies (Campbell et al., 2014; Mundy et al., 2005; Welch and Bergmann, 1989).

Using fluorescence imaging, the effect of snow cover removal on algae was also assessed at the millimeter scale (Lund-Hansen et al., 2014). This study further confirmed a decrease in biomass in areas with no snow due to possible increased UV light exposure and discussed the possible role of algae behavioral changes such as emigration under potentially photo-damaging conditions rather than ablation loss.

In the Antarctic, wind-driven snow re-distribution has been suggested as an important factor masking snow depth-biomass relationships (Melbourne-Thomas et al., 2015). In fact, the snow cover present on the ice at the time of sampling does not necessarily reflect the conditions during the earlier stages of ice development. This is particularly true for Antarctic sea ice where snow is a prominent feature, and continuous drift provides a rapidly changing snow cover and under-ice light conditions (Massom et al., 2001). Compared to the Arctic, studies emphasizing snow-biomass relationship in the Antarctic are less frequent, and the complex response of ice algal growth, photo-physiology, and distribution under changing snow and light fields requires further research efforts through higher spatial and temporal resolution monitoring and on both land-fast and pack ice.

Finally, is worth noting that since ice algae are commonly distributed in distinct layers that can reach several centimeters in thickness, and can exhibit diverse vertical distributions over the ice thickness, they can further influence light availability to the nearby and underlying communities in the ice column through a phenomenon known as self-shading (Kirk, 2011; Cota and Smith, 1991; Johnsen and Hegseth, 1991). Self-shading can limit algal growth, influencing patchiness, induce packaging effects (Wongpan et al., 2018; SooHoo et al., 1987) and is represented in Figure 2 as an internal loop within biomass variability.

2.5 Grazing

A challenging loss-term to account for in biomass variability is grazing by under-ice fauna and zooplankton (Werner, 1997; Welch and Bergmann, 1989, Figure 2). It is speculated that feeding dynamics of the under-ice realm might, however, contribute to the mesoscale variability of

measured ice algal abundance (Gradinger and Bluhm, 2004; Michel et al., 2002; Werner, 1997). More investigation over different seasons and on different types of ice covers are required to enhance our understanding of grazing impacts on ice algal biomass distribution. Furthermore, physical properties of different ice types such as ice texture and porosity are also suspected to impact on predator-prey interactions in the sea-ice brine channel system (Krembs et al., 2000). For example, larger predators can be excluded from brine channels depending on the architecture of the channel network. Smaller channels may provide refuge space but may be unfavorable for algal growth due to limitations in diffusive transport of nutrients (Krembs et al., 2000).

2.6 Regional characteristics

As schematized in Figure 2, all the parameters described above are highly dependent on the season, meteorological conditions and in particular on the geographic region that shapes the sea-ice physical environment (Petrich and Eicken, 2009; Eicken et al., 1991). Indeed, not only is the horizontal distribution of sea-ice algae naturally related to latitudinal gradients in solar irradiance (Raymond et al., 2009; Cota and Smith, 1991), but other unique regional features will also affect the distribution of ice algae. For example, freshwater drainage from melt ponds and nearby river discharges can both remove or inhibit the algae growth at the sea-ice-water interface through physical disturbance and exposure to freshwater (Rysgaard et al., 2001). In areas affected by warm Atlantic water inflow, bottom ice ablation, which deteriorates the ice algal habitat, is suggested to be a limiting factor for Arctic ice algal biomass build-up (Leu et al., 2015). In the Antarctic, loss of algae from underneath the ice has been linked to the effect of underwater currents at specific locations (Ryan et al., 2006a). Another example are the hemispheric differences between Arctic and Antarctic sea ice, as these display very different vertical distribution patterns and total biomass values (Arrigo, 2014; Arrigo et al., 2010; Spindler, 1990). For instance, surface flooding and snow-ice formation is a characteristic feature of Antarctic pack ice (Kattner et al., 2004), whereas melt ponds are a predominant feature of Arctic sea ice.

The two polar regions can exhibit very different types of ice algae communities (Leeuwe et al., 2018). A feature of the Antarctic is the occurrence of platelet ice which hosts very high ice algal biomass(Arrigo, 2017). Platelet ice consists of thin ice plates in the water column below the sea ice which largely increases the surface area for the ice algae to colonize, and with direct access to nutrients in the water (Arrigo, 2014). Ice platelets accumulate loosely under, or occur frozen into, the bottom of sea ice resulting in a highly porous and productive ice algae habitat (Arrigo et al., 1995). Platelet ice is associated with supercooled Ice Shelf Water, and its occurrence is generally limited to specific areas across the Antarctic continent (Langhorne et al., 2015). Nonetheless, platelet ice communities are considered of high importance, as any change in the highly productive platelet ice habitat in a warming ocean can have consequential effects across the rest of the Southern Ocean ecosystem (Langhorne et al., 2015). A feature more common to the Arctic, is the colonial diatom, *Melsosira arctica* which can form strands attached to the ice and suspended into the water column. By living suspended into the upper ocean, they can consume nutrients directly from the water column (Arrigo, 2014).

Non-polar sea ice such as found in the Baltic Sea or Saroma-ko lagoon (Northern Japan) also presents particular characteristics in algal biomass spatial variability with reported observations of variability to be negligible at scales < 20 m despite evident variations in snow depth (Granskog et al., 2005; Robineau et al., 1997). For more detailed information on differences in ice algal communities from Arctic, Antarctic and sub-Arctic areas we refer to recent reviews by Arrigo (2017) and Kaartokallio et al. (2017).

3 Concepts of bio-optics and radiative transfer in sea ice

The layered sea-ice matrix, here comprising snow and ice (and the water below) is characterized by the inclusion of brine and air pockets, precipitated salts, dust and sediments, algae, heterotrophic organisms, dead organic particulate material (detritus) and CDOM (Figure 3). As in any remote sensing application, the medium between the sensor and the light-interacting object will have an impact on the measured signal. A brief overview of the path that light traverses before reaching hypothetical sensors placed underneath the ice is essential for adequately applying and developing close-range under-ice optical remote sensing methods. A comprehensive introduction to radiometry and hydrologic optics can be found in (Kirk, 2011) and to the optical properties of sea ice and snow in Perovich (2017, 1996) and Warren (1982).

3.1 Basic elements of close-range under-ice optical remote sensing of algal biomass

Recent studies have reported empirical correlations between traditional ice-core chl-*a* measurements and under-ice spectral signatures for both the Arctic (Campbell et al., 2015, 2014; Mundy et al., 2007) and Antarctic (Wongpan et al., 2018; Meiners et al., 2017; Melbourne-Thomas et al., 2015). The most basic application of the technique involves the deployment of upward-looking hyperspectral radiometers under the ice at close distances (0.15—0.6 m) using L-shaped deployment arms (Lange et al., 2016; Melbourne-Thomas et al., 2015) (Figure 4a). To correlate the transmitted spectra with chl-*a*, traditional ice cores are then collected just above the radiometer measurements, and fluorometric estimates of chl-*a* are performed in the laboratory from the melted cores using standard methods

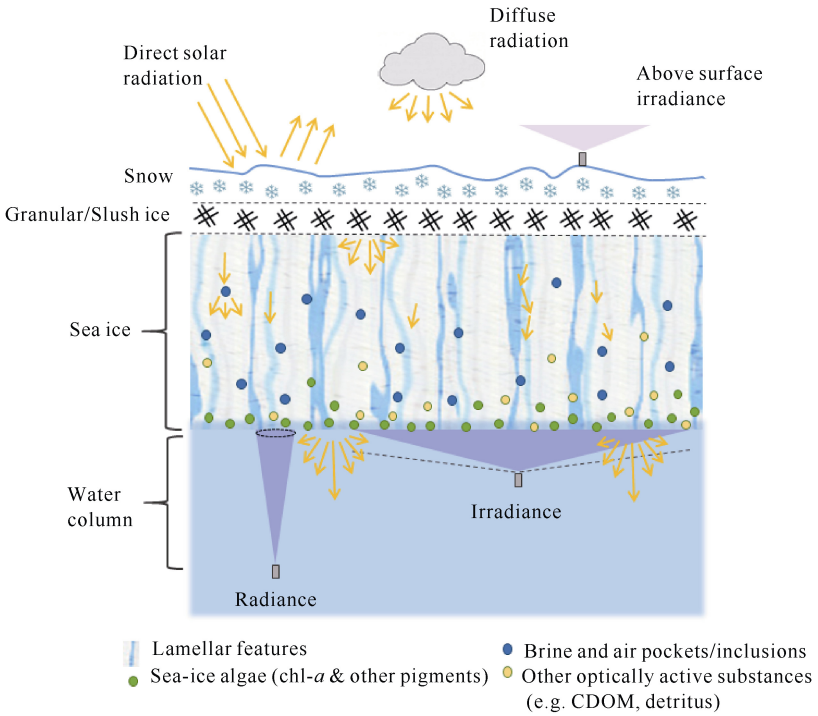

Figure 3 Conceptual illustration of radiative transfer in sea ice (for shortwave radiation between 350 and 700 nm) as described in text. The complex system features both absorbing and scattering elements that shape the geometric and spectral properties of the under-ice light field. The illustration provides a concept idea of typical under-ice light sensor settings employed for close-range remote sensing applications. Radiance sensors have a finite angle of view and are intended for finer mapping resolutions and deeper deployment modes (2—5 m). Irradiance sensors have to be deployed nearby the ice sub-surface due to their cosine field of view. Figure was partially adapted from Katlein et al., 2014.

(Holm-Hansen and Riemann, 1978) (Figure 4a). The technique takes advantage of the wavelength specific absorption of chl-*a*, with peaks at around 480 and 665 nm, and being the dominant absorbing pigment in ice algae. Measured transmitted spectra at multiple points are then calibrated against the sampled chl-*a* values through the use of derived spectral indexes or other regression models. Additional measurements of under-ice spectra can then be used to estimate chl-*a* concentrations using the radiometer data alone (Lange et al., 2016; Melbourne-Thomas et al., 2015). The spatial coverage of the survey can then be considerably increased by using Remotely Operate Vehicles (ROVs) or ship-based under-ice trawls equipped with the radiometric sensors (Meiners et al., 2017; Lange et al., 2016). Hyperspectral radiometers employed under sea-ice typically collect light in either irradiance or radiance mode (Figure 3). Irradiance sensors have a cosine-corrected receptor which gathers light with a 180° field of view (FOV). Radiance sensors have a narrow (finite) FOV (usually around 9° to 25°). While irradiance sensors provide a coarser footprint and are more frequently used for energy budget purposes, radiance sensors are used to infer optical properties at finer scales due to their narrow FOV (Lange et al., 2016). Figure 3 displays the hypothetical FOV coverage of both types of sensors. The transmitted under-ice light can be normalized with data from upward-looking irradiance sensors placed at the ice surface (Figure 3) (Nicolaus et al., 2010). Under-ice irradiance relative to incoming solar irradiance at the surface is termed transmittance whereas under-ice radiance normalized to incoming solar irradiance is termed transflectance (Nicolaus et al., 2013).

3.2 Scattering and absorption in sea ice

The attenuation through the ice, comprising both absorption and scattering, is typically expressed by the diffuse attenuation coefficient K_d (PAR) or spectrally resolved K_d (λ) (Lund-Hansen et al., 2015; Perovich, 1989). Both scattering and absorption govern the magnitude of the attenuation, but only the latter is considered wavelength dependent (Perovich, 1996; Arrigo et al., 1991). Scattering in sea ice depends on the scattering volume function, which is dominant compared to absorption, and is mostly attributed to the refraction of photons traveling between the different media such as ice, gas or brine inclusions and precipitatedsalts (Light et al., 2004; Perovich, 1996). Through continuously varying temperature gradients, the volume fractions of these optical media are far from being constant. Indeed, as a consequence of a dynamic physical environment, light attenuation and optical properties in sea-ice are continuously varying over space and time (Light et al., 2004; Perovich, 1996; Arrigo et al., 1991).

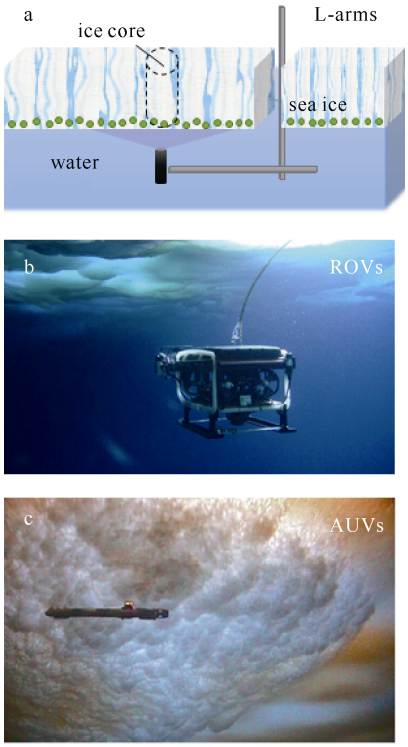

Figure 4 Traditional and emerging deployment modes for under-ice optical sensors. **a**, L-arms have been the starting point for acquiring under-ice spectral radiometric measurements due to their low-cost and relative ease of applicability; **b**, ROVs are emerging as a versatile tool to cover larger profiling transects compared to L-arms. The panel displays the Australian Antarctic Division's ROV under Antarctic sea ice (photo credit: Ulrich Freier); **c**, Autonomous Underwater Vehicles (AUVs) have not yet been employed for such type of applications due to the challenges described in the text. However, they present the potential to become a powerful tool towards large-scale mapping of biomass and method automation. The panel displays the GAVIA AUV under algae-populated Antarctic fast ice (photo credit: Vanessa Lucieer).

If we describe the light path starting from the surface, snow has a high albedo in the PAR range and the amount of light reflected is dependent on the conditions of the overlying snow cover (type, age, and temperature) (Perovich, 2007; Warren, 1982). Snow cover conditions are critically important as the overall amount of light transmitted/attenuated through the sea-ice matrix is mostly dependent on the thickness of the snowpack, rather than the ice, as snow attenuates light approximately 10-fold higher (Perovich, 2007).

If no snow is present, light transmission is mostly influenced by the surface properties of the sea-ice environment such as on the presence of melt-ponds or bare ice (Katlein et al., 2015a; Mundy et al., 2005). In Antarctica, thicker snow packs can induce surface flooding (Wadhams et al., 1987) which has been shown to slightly increase attenuation compared to non-flooded sea ice (Arndt et al., 2017). The authors hypothesized that although the different geometry of the slush layer allows more light to be transmitted, the higher snow loads and the promotion of infiltration waters (fostering algal communities living at the surface) resulted in the increased attenuation (Arndt et al., 2017).

Continuing downwards through the ice cover, absorption in sea-ice is often dominated by ice algae (Fritsen et al., 2011, 1992) and is enhanced by the highly scattering sea-ice environment they are embedded in (Ehn and Mundy, 2013). Here we focus on the 400 – 700 nm wavelength band termed the Photosynthetically Active Radiation (PAR), which is the spectral range relevant for under-ice optical remote sensing of biomass. Below 570 nm, absorption of snow and ice is low, and therefore ice algae dominate the spectral signature of transmitted light which is shaped by algae absorption features (Fritsen et al., 2011). This is what makes under-ice optical remote sensing methods possible. The spectral signature measured underneath the ice is dominated by effects associated with variability in algae absorption over certain bands of the PAR spectrum, rather than variability in snow and ice properties.

The irradiance that reaches the ice-water interface can be reduced to 0.1%—1% of the surface irradiance (Perovich, 2017; Fritsen et al., 2011), and thus the under-ice realm can be thought of as a low light environment. Nevertheless, ice algae can shade-adapt efficiently to these circumstances, and a recent Arctic study showed that active photosynthesis can occur at extremely low irradiances (0.17 $\mu M \cdot m^{-2} \cdot s^{-1}$) equal to 0.02% of surface irradiance (Hancke et al., 2018).

Overall, the quantification of the effects of algal biomass on the optical properties of sea-ice is non-trivial. The quality of the light is influenced by the amount of chl-*a*, but it also varies as a function of algal photosynthetic and accessory pigment composition within the algal cells, as well as with the effect of photosynthetic discreteness which combines the influence of size and of pigment concentration in the cells (e.g., packaging effect) (Kirk, 2011; SooHoo et al., 1987; Morel and Bricaud, 1981). For example, the specific absorption of the ice algal community varies as a function of the diverse photoacclimation strategies of ice algae adapted to different light levels. These can induce the production of diverse cellular pigment compositions (Galindo et al., 2017), which can lead to distinct spectral absorption profiles (Johnsen and Sakshaug, 2007).

Although spectrally resolved visible light signals measured below the ice are mostly shaped by absorption of organic matter (algae and detritus) within the ice, the signal also comprises the absorption effect of other optically active components, and thus the discrimination of chl-*a* is not always straightforward. Chl-*a* has absorption peaks at around 480 and 665 nm, whereas CDOM absorption is strongest in the blue part of the spectrum (400—450 nm), but low in the red. In the red part snow absorption starts to increase (over 550 nm). The concentration and distribution

of other optically active components are dependent on the study region. Analyses of CDOM and its optical properties remain sparse but are available for both Arctic (Lund-Hansen et al., 2015; Xie et al., 2014) and Antarctic (Norman et al., 2011) sea ice.

3.3 Geometrical considerations of the under-ice light field

Considering the high scattering coefficients of snow, with only a few centimeters of snow cover, light that reaches the surface-ice layer is in an entirely diffuse form rendering the sun-angle induced directional component of light negligible (Petrich et al., 2012). A similar effect is achieved by the granular ice surface layers characteristics of melt (or flooding) and refreezing processes at the snow-ice interface (Petrich et al., 2012; Worby et al., 1998) or by overcast conditions.

Therefore, for most of the cases, light that reaches the ice sub-surface can be considered diffuse, and it follows an exponential decrease through the ice and thereafter through the water column (Lund-Hansen et al., 2015). Exceptions are made for non-homogenous ice in pond covered areas typical of the Arctic (Frey et al., 2011) or near ice floes with cracks and ridges which can include an azimuthal directional component in the under-ice light field measured nearby, and different depth profiles (Katlein et al., 2016, 2015a).

While light that has traversed the initial sea-ice surface layers results considerably scattered and diffuse, radiative transfer within sea ice is subject to a degree of substantial anisotropy and multiple scattering (Katlein et al., 2015a; Petrich et al., 2012). This means that the scattering coefficient is dependent on the direction in which light is traveling, which in turn is dependent on a volume scattering function (Hamre et al., 2004). The lamellar crystal structure of sea ice is responsible for such particular geometric and radiometric light field properties (Katlein et al., 2016; Perovich, 1989). More specifically, the sea ice vertical lamellar crystal structure, and brine and gas inclusions funnel the light downwards changing the shape of the radiance distribution under-ice to a downward-peaked shape along the zenith angular component (Figure 3) (Katlein et al., 2014; Light et al., 2004). This reduced lateral deflection within sea ice is further enhanced by absorbing particulates such as algae, detritus, dust and sediment (Petrich et al., 2012). The overall consequence of this phenomena is an anisotropic under-ice light field characterized by a narrowed spread of flux (Figure 3), which remains constant over time through various sea ice temperature regimes (Light et al., 2004).

In terrestrial remote sensing, an anisotropic light field is typically characterized by the bidirectional reflectance distribution function (BRDF) which defines the geometric radiance distribution (Palmer and Grant, 2010). The BRDF effect can hinder the retrieval of accurate information from remotely sensed data (Buchhorn et al., 2016). Measurements obtained by an under-ice sensor are inevitably subject to such considerations as well. The impact of an anisotropic under-ice light field should be subject of further investigation towards the development of accurate under-ice light measurements that aim to be flexible regarding sensor characteristics and deployment mode (e.g., from underwater vehicles, using wide FOVs or HI comprising sensor inclination and multiple viewing angles). In addition, more studies analyzing the effect of different ice types and sea-ice surface properties on the under-ice lights field geometrical properties (e.g., surface flooding), are of interest for further extending under-ice chl-*a* remote sensing under a wide range of survey scenarios.

4 Advances in under-ice optical remote sensing of biomass

4.1 Regression algorithms

The first studies describing correlations between transmitted under-ice irradiance spectra and sea-ice chl-*a* were performed by Legendre and Gosselin (1991) and Maykut and Grenfell (1975). The studies employed ratios between selected spectral bands (671 nm : 540 nm) and produced a relationship accounting for up to 55% of total variation in ice algal biomass. Subsequent studies have employed Normalized Difference Indexes (NDIs) as a method to correlate under-ice spectra with sea ice algal biomass estimates in Resolute Passage, Canada (e.g., Mundy et al., 2007). The study pointed out the negligible effect of snow on biomass estimations if NDIs were calculated with wavebands where snow had reduced influence (<570 nm). The authors provide a single-best NDI wavelength combination (485 nm : 472 nm) accounting for 89% in the total variation of ice algal biomass. This study was complemented by two more Arctic studies (Campbell et al., 2015, 2014) also conducted in Resolute Passage. Taking advantage of the non-invasive nature of the method, the studies were able to infer algae environmental drivers (such as snow depth) and found the best NDI wavelength combination (478 nm : 490 nm) to account for 81% of sea ice chl-*a* biomass variability.

The same method was also applied in Antarctic pack ice, explaining 81% of algae biomass variability using the ratio of wavelengths (555 nm : 472 nm) (Fritsen et al., 1992). This was followed by the first study comparing data from different locations on a regional scale (Melbourne-Thomas et al., 2015). The later tested different types of spectral feature models (NDIs, ratios of spectral irradiance, scaled band area, and Empirical Orthogonal Functions, EOFs) and highlighted NDIs to be the most effective index accounting for biomass variation (Melbourne-Thomas et al., 2015). Different optimal NDI wavelengths were identified for East Antarctic sea ice (422 nm : 418 nm) and the Weddell sea ice (479 nm : 468 nm) (Melbourne-Thomas et al., 2015). Generally, best NDIs are selected by plotting Pearson correlation surfaces which display correlation strengths among all combinations of spectral wavebands

(each combination produces an NDI) (e.g., Melbourne-Thomas et al., 2015). NDIs should, however, be composed of wavebands that are separated by at least 15 nm to avoid artificial correlations of neighboring wavebands and, for chl-*a*, preferably wavelengths between 405 and 550 nm to avoid both edge effects and the influence of snow on transmitted radiance spectra beyond 550 nm.

It is important to note that all these tests have only used irradiance sensors at a very close distance to the ice subsurface (0.15—0.6 m), providing scattered point samples over limited areal extents. The first comparison of algorithms to include long-range transects using radiance sensors was conducted by Lange et al. (2016) for Arctic sea ice. The study examined different regression models (EOFs, NDIs, and Multi-NDI) and observed a better performance for the EOFs-based approach to represent increased areal coverages (therefore representing a more extensive range of sea-ice conditions). Also, this study outlined that a better model performance can be achieved by using transmittance or transflectance data as spectral model inputs rather than only under-ice irradiance or radiance data. Studies testing and comparing different models under different conditions are useful for progressing more generalized relationships and robust regression models. The latest study investigating under-ice spectra- biomass relationships was done in Antarctic fast ice, and it showed that NDI wavelength pairs near the first chl-*a* absorption peak (440 nm) explain up to 70% of the total variability in high ice algal standing stocks (Wongpan et al., 2018). The authors also pointed out the importance and difficulty of sampling on one of their study areas, McMurdo Sound, characterized by the presence of platelet ice. The sub-ice platelet layer is characterized by one of the highest biomass concentrations. However, the produced relationships in the study were hampered by a low overall variability in the sampled algal biomass and the potential biases in sampling the fragile unconsolidated sub-ice platelet layer. The authors highlighted that further work is required to advance quantitatively robust sampling techniques for platelet ice and to develop optical methods to understand phenology and spatial variability of platelet ice algal communities.

Table 2 provides a summary of the studies producing spectra-biomass relationships retrieved from the close-range deployment of radiometers. The differences in optimal spectral indices and produced relationships suggest that it is challenging to develop cross-regional relationships between transmitted spectra and chl-*a* (Wongpan et al., 2018; Melbourne-Thomas et al., 2015). The differences in sea-ice physical properties, in algal community composition and photophysiological adaption strategies, together with the spatio-temporal variability impedes the formulation of a universal relationship. This is particularly true if relationships are derived from univariate statistical models. In fact, Lange et al. (2016) pointed out that the EOF approach provided better correlations because it accounted for a broader range of spectral variability by including multiple regions of the spectra.

Table 2 Compilation of studies using measured under-ice spectra for estimating chl-*a* (in mg·m^{-2}) in sea ice. All studies correlate optimal spectral bands with measured chl-*a* obtained through traditional ice coring techniques. Location, ice type and date of the survey are shown together with the method employed, produced relationships and the statistical strength of the correlations as R^2. *Sba* refers to the scaled band area found in the respective studies. *S* refers to the EOF scores found in the respective studies. *E*(chl-a_{adj}) indicates that a log-link function was applied for the formulation of the relationship. ln indicates that a natural logarithm was employed to formulate the relationship. Sensor mode refers to the FOV (radiance or irradiance) and if it was normalized to downwelling surface radiation (transflectance or transmittance)

Study	Region/Ice type/Date	Method used/Optimal bands (if any)/Sensor mode	Relationship	R^2
Legendre and Gosselin, 1991	• South-eastern Hudson Bay, Canadian Arctic • FYI • May 1986	*Ratios* 671:540 Irradiance	chl-*a* = 100 × ratio + 49	0.55
		NDIs 415:400 Transmittance	chl-*a* = 80.2 − 588 × *NDI*	0.81
Mundy et al., 2007	• Resolute Passage, Canada • Land-fast FYI • May 2003	*NDIs* 485:472 Transmittance	chl-*a* = −8.3 + 1000 × *NDI*	0.89
		NDIs 663:655 Transmittance	chl-*a* = −26.72 + 344 × *NDI*	0.85
		NDIs 685:675 Transmittance	chl-*a* = 43.87 + 204 × *NDI*	0.81

Continued

Study	Region/Ice type/Date	Method used/Optimal bands (if any)/Sensor mode	Relationship	R^2
Campbell et al., 2015, 2014	• Allen bay. Northwest of Resolute Bay, Nunavut, Canada • Land-fast FYI • May—June 2011	*NDIs* 478:490 Transmittance	chl-*a* = −497.2 × *NDI* + 15.2	0.81
Fritsen et al., 2011	• Bellingshausen Sea • FYI • September 2007	*NDIs* 555:442 Irradiance and transmittance	n/a	0.71(for irradiance) 0.81(for transmittance)
		NDIs 422:418 Irradiance	ln(chl-*a*) = −4.27 – 351 × *NDI* (for East Antarctica)	0.64
		NDIs 479:468 Irradiance	ln(chl-*a*) = 0.39 + 31.7 × *NDI* (for Weddell sea, updated with corrigendum)	0.79
		Ratios (555:443) Irradiance	ln(chl-*a*) = −1103 + 1948 × Ed(555)/Ed(443) − 859 × [Ed(555)/Ed(443)]^2 (for East Antarctica)	0.56
Melbourne-Thomas et al., 2015	• Antarctic sea ice. Weddell Sea and East Antarctica • Pack-ice (Ice floes) • September—October 2007—2012	*Ratios* (555:443) Irradiance	ln(chl-*a*) = − 33.9 + 31.0 × Ed(555)/Ed(443) (for Weddell sea)	0.67
		Scale band area Irradiance	ln(chl-*a*) = −16.36 + 9.52 × *sba* − 1.34 × *sba*^{2} (for East Antarctica)	0.64
		Scale band area Irradiance	ln(chl-*a*) = −2.40 + 1.64 × *sba* − 0.13 × *sba*^{2} (for Weddell sea)	0.60
		EOFs Irradiance	ln(chl-*a*) = 0.36 + 6.41 × S_1 − 143.5 × S_2 − 20970 × S^2_2 + 393.3 × S_3 − 512.6 × S_4 (for East Antarctica)	0.52
		EOFs Irradiance	ln(chl-*a*) = 1.55 + 43.0 × S_1 + 112.5 × S_2 − 243.7 × S_3 (for Weddell sea)	0.67
Nicolaus and Katlein, 2013	• Barrow, Alaska, Arctic sea ice • Land-fast sea ice, snow covered • March, May, and June 2010	No correlation could be applied.	n/a	n/a
Lange et al., 2016	• Central Arctic Ocean • Different ice types from ponded ice, snow, and ponds frozen, no snow and ponds, frozen surface (FYI, MYI) • August—October 2011	*NDIs* 669:683 Irradiance	ln[*E*(chl-a_{adj})] = 2.2 + 10.8 × *NDI*	0.73
		NDIs 678:684 Transmittance	ln[*E*(chl-a_{adj})] = 1.2 − 11.1 × *NDI*	0.70
		EOFs Transflectance	ln[*E*(chl-a_{adj})] = 0.3 + 1.5S_2 − 1.7S_4 − 2.0S_7 + 3.2S_9 + 8.6S^2_9	0.74
		EOFs Transmittance	ln[*E*(chl-a_{adj})] = 0.7 − 3.0S_2 + 1.1S_4 + 2.4S_6 − 6.5S^2_7 + 3.9S^2_9	0.90
		EOFs Radiance	ln[*E*(chl-a_{adj})] = 2.0 + 2.7S_4 − 1.7S_5 − 1.0S_6 − 2.3S^2_2 − 10.0S^2_8	0.95

Continued

Study	Region/Ice type/Date	Method used/Optimal bands (if any)/Sensor mode	Relationship	R^2
Meiners et al., 2017	• The Weddell Sea • Pack ice floe • September 2017	*NDIs* 479:468 Irradiance	ln(chl-*a*) = 0.39 + 31.7 × *NDI* (from Melbourne-Thomas et al., 2015)	0.79
Wongpan et al., 2018	• Antarctic sea-ice, McMurdo Sound and Davis Station. • Fast ice (First-year) • Austral spring 2015	*NDIs* 471: 416 Transmittance	$\log_{10}$(chl-*a*) = 1.27 + 3.763 × *NDI* (for McMurdo Sound)	0.07
		NDIs 439: 424 Transmittance	$\log_{10}$(chl-*a*) = 2.07 – 18.163 × *NDI* (for Davis Station)	0.79
		NDIs 441: 426 Transmittance	$\log_{10}$(chl-*a*) = 2.58 – 16.85 × *NDI* (for both sampling sites)	0.70

Different types of sea-ice cover at different locations over different seasons control algal community composition, biomass accumulation and ice algal bio-optical characteristics (Galindo et al., 2017; AlouFont et al., 2013). As an example, low light availability may trigger shade acclimation leading to an increase in the chl-*a* per cell ratio and increased production of accessory pigments, thereby boosting the ice algal package effect (decreased absorption efficiency per chl-*a*) (Wongpan et al., 2018; Melbourne-Thomas et al., 2015; Kirk, 2011). Theoretically, the effect induces a flattening of the absorption spectrum of the bulk algae composite (Morel and Bricaud, 1981) and could consequentially result in an underestimation of chl-*a* due to the presence of other ice algal pigments such as fucoxanthin and diadinoxanthin, affecting absorption but not chl-*a* concentration.

Also, it has been shown that the absorption spectra of algal communities change vertically over the sea-ice cover (Fritsen et al., 2011). Due to different light levels, ice physical properties, and nutrient availability along the vertical gradient in the sea ice, algae communities at different depth layers will adopt distinct acclimation strategies which have an impact on their pigment composition which can affect absorption spectra (AlouFont et al., 2013). Even though populations are generally found at the bottom of the ice, the effect of different vertical distributions and diverse species composition on the optical method has not been assessed and requires further investigation.

In this context, future studies should include pigment determination using High-Performance Liquid Chromatography (HPLC) to measure the entire suite of photosynthetic and photoprotective algal pigments (Miller et al., 2015), and measurements of particulate and algal absorption spectra using spectrophotometers equipped with integrating spheres (Wongpan et al., 2018; Lund-Hansen et al., 2014).

Another limitation of the described optical method is related to the minimum amount of chl-*a* in the ice that can be detected by under-ice remote sensing (Lange et al., 2016; Nicolaus et al., 2013). Studies have attempted to correlate fluorometric chl-*a* estimates with under-ice spectra without success. This has been attributed either to low algal biomass or the high concentrations of other substances in the few cores sampled for cross-calibration (Nicolaus et al., 2013; Nicolaus and Katlein, 2013). With low chl-*a* concentrations in the ice, the correlations are dominated by effects of other optically active components and hinder the development and establishment of accurate models.

Nevertheless, whilst the strength of correlation within the models is noticeably variable (Table 2), opportunities for improvement for model robustness exists. From a remote sensing perspective, the goal is to provide more accurate correlations able to determine chl-*a* from spectral data and other remotely sensed physical parameters without the need to calibrate with local chl-*a* measurements for every single survey. So far, mostly univariate models have been tested, and further research could be conducted in this area with regression models attempting to take advantage of multiple spectral bands or additional parameters as shown in studies on other targets (Liu et al., 2011). There is an extensive library of algorithms available that could be tested for developing improved relationships between measured spectra and sampled chl-*a* (e.g., in the field of machine learning). Adequate algorithms can be selected based on the amount of data available and characteristics of the algorithm with references from comparable studies applied in remote sensing of other environments. For example, studies have successfully estimated biomass in wheat employing multiple univariate indexes as input parameters for different machine learning models such as random forest or artificial neural networks (Wang et al., 2016). In the case of sea-ice algae, different statistical indexes such as NDI, ratios, scaled band area, and EOFs can be tested together as model parameters potentially providing more robust regression models. The reasoning behind this is that the different properties of some indexes are more capable of accounting for specific differences in the sea-ice environment, resulting in overall more robust models (Lange et al., 2016; Melbourne-Thomas et al., 2015).

To overcome regional dependence, predictive statistical models could be trained over the acquired high spectral and spatial resolution datasets for developing regressions models using diverse input parameters such as the hyperspectral data, ice thickness, snow depth, sub-surface roughness, geographical location and proxies of algal photoadaptation among others. The scheme of environmental drivers in Figure 2 suggests some possible parameters, representative of fine and large-scale processes, which could be used in the parametrization of new predictive models.

The problem for sea ice training datasets is that they are generally scarce due to the remoteness of the study areas and the difficulty of sampling sea ice. New, more robust algorithms will require considerable amounts of data and variables to develop accurate predictions. Producing datasets coupling physical and biological parameters would not only assist in a better understanding of the natural process governing algae distribution but could also provide indicators useful for modeling the relationships. In this context, future chl-*a* sampling campaigns should be, when possible, paired with under ice spectral measurements, proxies of algae photophysiological adaptations and other parameters to create an extensive cumulative dataset over time and for multiple ice types.

4.2 Possibilities beyond biomass regression models

Outside the range of statistical regression models, hyperspectral data may also improve our understanding of sea-ice algae beyond simple biomass distribution estimates. This might include the possibility of discretely distinguishing algae physiological conditions (e.g., Perkins et al., 2016) and detection of community compositions from the under-ice signals as analogously done in phytoplankton and vegetation studies (Zhang et al., 2015; Moisan et al., 2011). This could be achieved through hyperspectral signal decomposition and analyses aimed to resolve relative amounts of different types of algae pigments, CDOM or other detritus presence. Hyperspectral and multispectral airborne data have been used to estimate pigment composition of terrestrial plants for example (Blackburn, 2006). The differentiation between algae species in sea ice is important for improving the understanding of ice algal primary productivity, phenology and in support of predictive modelling efforts (Leu et al., 2015; Lizotte, 2001). For this purpose, different spectral decomposition techniques could be tested a priori through laboratory approaches with known algae species and concentrations in controlled environments (e.g., Mehrubeoglu et al., 2013; Moberg et al., 2002).

4.3 Under-ice platforms for sea-ice radiation transfer mapping

Accurately mapping spectrally-resolved under-ice shortwave radiation with high-frequency point sampling is paramount for the development of under-ice optical remote sensing methods aimed to improve biomass spatial variability estimates in sea ice. In this context, UUVs and trawl based system are showing high capabilities to survey under-ice areas in a spatially and temporally efficient manner where usually difficult access is the norm (e.g., Lange et al., 2016). UUVs include both ROVs (Figure 4b) and AUVs (Figure 4c). A general overview on UUVs describing each platform type, potentials and limitations is given in Wynn et al. (2014), and a description of their differences and complimentary use for scientific operations by Ludvigsen et al. (2013).

Radiance and irradiance hyperspectral radiometers mounted on ROVs have recently been deployed for mapping under-ice radiation transfer under both Arctic land-fast and a pack ice (Lund-Hansen et al., 2018; Katlein et al., 2015a; Nicolaus et al., 2013; Nicolaus and Katlein, 2013), and under Antarctic pack ice (Arndt et al., 2017; Meiners et al., 2017). Table 3 provides a compilation of all studies employing UUVs for under-ice radiation transfer mapping. Surveying transects up to 150 m long and areal point sample grids up to 100×100 m^2 have been measured. For sea ice, the use of remotely operated platforms also solves issues related to the bias of sampling towards stable ice floes due to the practical and safety requirements associated with deploying personnel for ice coring. Sampling with remotely operated platforms allows researchers to efficiently survey various types of sea ice, such as newly formed ice, ponded ice as well as snow-covered sea ice and pressure ridges within the same survey. For these first approaches, vehicle depths have ranged from 1 m to a maximum of 10 m from the ice sub-surface (Table 3). However, data are typically filtered so that only spectral measurements within 2 m from the ice bottom are accounted for. An exception is for Lund-Hansen et al. (2018) which successfully developed and deployed and ROV for measuring under-ice irradiance fields, sliding at a fixed distance of 0.25 m between the ice bottom and sensor head, using spacer poles.

Compared to under-ice L-arm measurements, UUVs introduce a higher degree of complexity in terms of sensor settings, specifications, and deployment. Particularly if these are to be operated at increasing water depths and in a dynamic setting. Figure 5 summarizes all components that require consideration when performing under-ice studies employing UUVs and spectral radiometers. There are trade-offs between the typical remote sensing ambitions and the technical and environmental constraints of the survey.

For example, signal to noise ratio (SNR) is a primary parameter for evaluating hyperspectral data quality (Adão et al., 2017). As underwater platforms are constantly in motion, they require shorter integration times to avoid blurred/displaced sensor footprints (e.g., Lange et al., 2016), with concomitant implications for the SNR (less light gathered per sample) (Figure 5). Also, as vehicle distance from the ice increases, the sensor footprint widens, and the

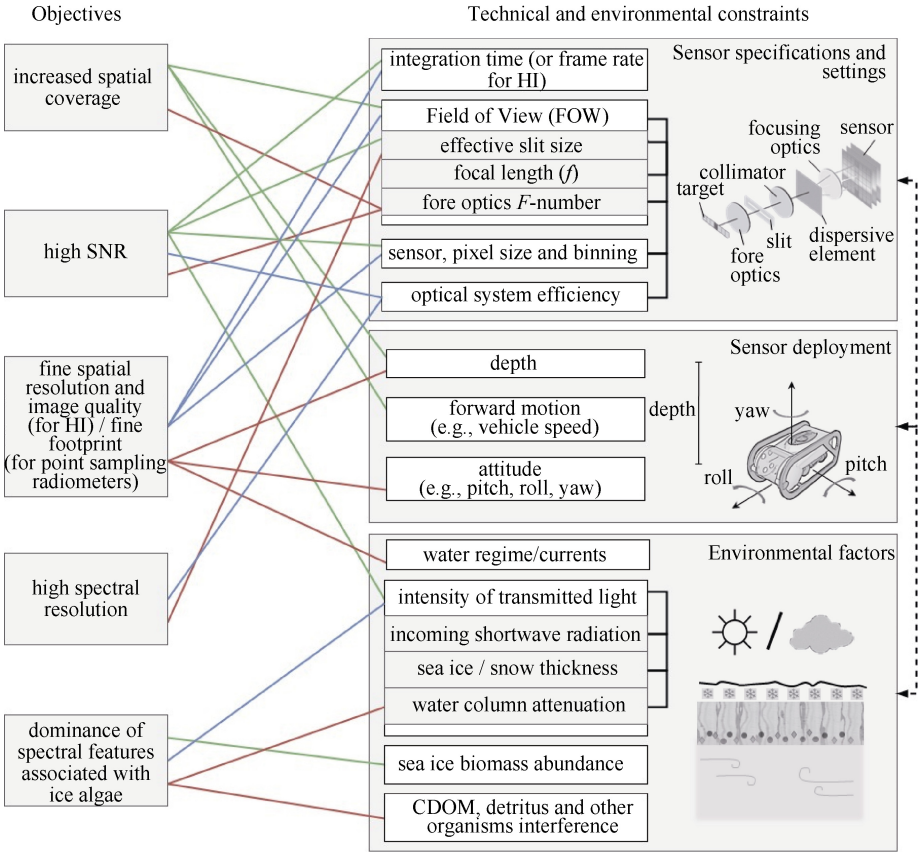

Figure 5 Schematic of the trade-offs between the typical remote sensing objectives (left), and the technical and environmental factors to consider in an under-ice surveying context. Red links indicate that there is an inverse relationship between the ideal objective and the factor whereas green links indicate a positive relationship. Blue connectors refer to a variable relationship. The black line connectors indicate that the factors are highly correlated. More information can be found in the text. Overall, sensor specifications need to be set according to deployment mode and to the environmental constraints (symbolized by the black dotted line). The optical system efficiency includes optical throughput of the lenses, the dispersive element efficiency, and the detector quantum efficiency. The scheme is valid for both non-imaging radiometers and HI. Spatial resolution refers to the ground sample distance of an imaging spectrometer. The spatial footprint refers to the circular footprint of normal spectrally resolved radiometer. SNR refers to Signal to Noise Ratio.

Table 3 A compilation of published studies employing UUVs or any other kind of underwater platform (e.g., under-ice sleds or under-ice trawls) for radiation transfer mapping under sea-ice

Study	Region/Ice type/Date	Platform and sensor	Survey information
Lange et al., 2016; Nicolaus and Katlein, 2013	• Central Arctic Ocean • Different ice types from ponded ice, snow and ponds frozen, no snow and ponds, frozen surface (FYI, MYI) • August—October 2011	ROV. Radiance and irradiance sensors (TriOS, RAMSES-ACC/ARC)	Various transects of 30 to 210 m. Depths from 1 to 10 m. Filtered to <1.5 m for biomass estimates.
		Under-ice trawls. Radiance and irradiance sensors (TriOS, RAMSES-ACC/ARC)	Two transects of 800 and 1500 m respectively. Depths from 0 to 200 m. Filtered to <1.5 m for biomass estimates.
Nicolaus et al., 2013	• Barrow, Alaska, Arctic Ocean • Land-fast sea ice, snow covered • March, May, and June 2010	Under-ice sled. Irradiance (TriOS, RAMSES ACC)	Three transects of 20, 40 and 80 m. No depth. Spectroradiometer at 2±1 cm from the ice subsurface.
Katlein et al., 2015a	• Arctic Ocean • Ice floe with melt ponds • July 2014	Nereid Under Ice (NUI) (hybrid ROV). Radiance and Irradiance (TriOS, RAMSES-ACC/ARC)	100 m transects at approx. Depths of 5 m.
Arndt et al., 2017; Meiners et al., 2017	• Weddell Sea • Ice floe of flooded pack-ice • September 2013	ROV, Irradiance (TriOS, RAMSES-ACC)	100 m-by-100 m grid. Depths filtered to < 2 m.
Lund-Hansen et al., 2018	• Kangerlussuaq, West Greenland • Landfast first-year ice • March 2016	Low-cost portable ROV. Irradiance (TriOS RAMSES ACC-UV/VIS)	15 m transects. Sensor fixed depth of 0.25 m.

resolution of the survey data will decrease (e.g., will become coarser). Constantly moving vehicles deployed at specific depths will by necessity make a trade-off between spatial footprint resolutions, integration times and quality of the signal (Figure 5). While some of these underwater vehicles allow for longer integration times by moving at very slow speeds or hovering/parking in a relatively fixed position (e.g., ROVs), other approaches such as the ship trawls or modern AUVs are limited in this aspect. Furthermore, sensor integration times need be set according to the continuously varying environmental conditions such as daylight availability, the sea-ice physical properties (e.g., ice and snow thickness controlling total under-ice irradiance levels) and the water column properties (e.g., destabilizing currents or other optically active materials in the water) (Figure 5). While there would be no "best" setting for every surveying scenario, as this will depend on the sea-ice conditions, desired spatial-sampling resolutions and equipment availability, surveys benefit from stable ocean current conditions, clear waters and constant-upward looking sensor attitude.

Compared to ROVs, AUVs are underwater drones that are capable of executing pre-programmed routes to cover significant distances (10's of kilometers). Although there are no published studies employing AUVs for biomass estimates in sea ice except for a study by Forrest et al. (2016), AUVs are increasingly being used for sea-ice research and are showing great potential (Singh et al., 2017; Lucieer et al., 2016; Norgren and Skjetne, 2014; Williams et al., 2014). However, all the aforementioned problems would be accentuated when mounting sensors on AUVs due to the mechanisms for AUV operation. These include deeper operating depths to avoid collision hazards, constant but relatively fast traveling speeds, and geo-referencing the motion of the vehicle to the finely tuned sensors. When using irradiance sensors, increased distance to the ice sub-surface will lead to a strong areal averaging of light levels and a loss of spatial resolution (Figure 3). Therefore surveys would require radiance sensors to be deployed according to the desired mapping footprint by regulating vehicle depth based on the FOV of the sensor and vehicle capabilities. Radiance sensors with a narrow FOV are therefore fundamental if the sensor is to be deployed at increasing depths while still aiming to achieve specific mapping resolutions and to avoid the light influence of the surrounding water column (Nicolaus and Katlein, 2013). The trade-off with radiance sensors (and HI sensors) is that they are less sensitive compared to irradiance sensors since reduced collection angle inevitably results in a reduced amount of light collected per a defined integration time (Figure 5).

Furthermore, considering the anisotropic nature of the under-ice light field, sampling radiance distribution would not be accurate if the light field varies considerably across the field of view of the sensor as previously mentioned. This is because radiance sensors collect light from a finite solid angle (Figure 3), but radiance is mathematically defined for an infinitely small solid angle. Sensor settings and deployment mode would, therefore, need to be regulated for the desired outcome, considering the constraints outlined in Figure 5 as well as the under-ice geometric light field. Katlein et al. (2016) used a geometric light field model to investigate this aspect and suggested that radiance measurements (with a 10 degree FOV sensor) conducted more than 4 m away from the ice underside would need to be converted to under-ice irradiance using a conversion method based on the C value outlined in Katlein et al. (2014). The C value depends on the angular distribution of radiance underneath the ice and can be obtained from a direct measurement of the radiance distribution under the ice, or either from sea-ice physical properties. Considerable work is required to standardize the application of finite FOV sensors in under-ice remote sensing studies.

4.4 Hyperspectral imaging

Hyperspectral imaging (HI) aims to obtain the spectrum for each pixel in the image of a scene, with the purpose of finding objects, identifying materials, or detecting and quantifying processes (Bioucas-Dias et al., 2013). As the technology becomes more portable and accessible, it has found an immense range of applications ranging from environmental monitoring (Adão et al., 2017), chemometrics (Amigo et al., 2015), precision agriculture (Mäkynen et al., 2012), forensic analyses (Edelman et al., 2012) and medicine (Lu and Fei, 2014) to mention a few. Depending on the desired aims and settings, these sensors can capture features at different scales ranging from millimeter close-range imagery to continuous swaths of data at the mesoscale depending on the sensor distance from the target and the mounting platform.

The hyperspectral images consist of a three-dimensional (x, y, λ) data cube where x and y represent the spatial dimension (with pixel sizes that can vary depending on the survey type), and λ the spectral dimension. The modality in which the frame is acquired can be in either push-broom or snap-shot mode (e.g., Huang et al., 2014). Each type of sensor presents both advantages and disadvantages with the choice purely based on user preferences. HI data processing involves pre-processing of raw data cubes, compression, exploration, regression, and segmentation to finally providing abundance estimates or classification of the desired features (e.g., Amigo et al., 2015; Bioucas-Dias et al., 2013).

Application of HI in the underwater domain is relatively new and presents several optical and technical challenges that still require considerable research effort. However, pioneering studies are highlighting the potential for creating high resolution, georeferenced, optically corrected digital underwater maps of different habitats, minerals, substrates, and organisms (Dumke et al., 2018; Chennu et al., 2017, 2013; Johnsen et al., 2013).

A recent study assessed the use of HI for mapping

sea-ice algae biomass variability at the ice-water interface in an experimental sea-ice simulation tank (Cimoli et al., 2017a). Using a pushbroom hyperspectral camera at 1 m distance over a 0.72 m^2 ice surface, variability in ice algal biomass was captured in images at very high spatial resolutions (0.9 mm square pixels). The sensor acquired radiometric data over the PAR range (400—700 nm) and following repeated tests at multiple spectral resolutions the study concluded that spectral resolutions > 6 nm could not be suitable for ice algal habitat mapping. For an under-ice algal mapping context, the high spatial variability at the microscale, the varying photophysiological adaptations of ice algae (modifying absorption spectra), and the highly variable under-ice light environment need to be considered when selecting an HI sensor. Snapshot HI sensors are easier to use (more portable and not constantly requiring a set of six orientation parameters) than pushbroom sensors which require a relatively constant and accurate forward motion across the imaged target and are drift sensitive. Pushbroom sensors require the integration time (or frames per second) to be set according to the moving speed for reconstructing the images (Figure 5). The aim is to attain adequate SNR, and due to the finite number of pixels on a focal plane array, snapshot HI sensors make a trade-off in the resolution of the various dimensions of data of the data cube sacrificing either spatial or spectral resolution. This can be limiting depending on the surveyed target, the desired mapping resolution and in particular under low light conditions.

Analogously to standard point sampling radiometers, Figure 5 outlines for HI the relevant under-ice tradeoffs between the typical optical remote sensing ambitions that need to be balanced with both technical and environmental factors. For HI cameras, finer spectral resolution can be offset by a lower SNR when compared to multispectral sensors because of the fewer number of photons captured by each detector due to the narrower width of the spectral channels (Figure 5). Furthermore, SNR associated with this type of sensor are accentuated compared to standard radiometers due to the light redistribution across spatial pixels along the sensor. Such systems necessarily need to involve a more sensitive instrument set-up by considering deployment depth, integration times (or frames per second) and moving speeds (for pushbroom sensors) (Figure 5).

There is also a series of other technical considerations in HI sensor and settings selection. To mention a few, the fore-optics need to match the light collection capability of the diffracting element (Figure 5). If the lens' *F*-number is too low, the slit can overfill causing increased stray light (reduced SNR); if the *F*-number is too high, it will limit the throughput of the system (thus the SNR). On the other hand, the slit size of the instrument is inversely proportional to the spectral resolution of the system, but positively correlated with the amount of light reaching the sensor and thus also affect the SNR (Figure 5). Other technical sensor specific capabilities include pixel binning, which merges pixels to increase SNR at the expense of either spatial or spectral resolution, or the overall optical system efficiency and quality (Figure 5).

From a remote sensing perspective, the goal is to deploy sensors deeper (to increase the spatial footprint and areal coverage), to make them move faster (to reduce operational times and increase efficiency) and to capture as much light as the conditions allow. Eventually, HI technology could be routinely mounted onto UUVs as proposed for underwater benthic mapping (Johnsen et al., 2013) or deep-sea classification of features of interest (Dumke et al., 2018). However, there is a complex trade-off between all the aforementioned parameters that will need to be assessed for each case (Figure 5). Deployment of wide FOV sensors might be constrained due to under-ice anisotropic and surface dependent light fields (Katlein et al., 2016, 2014; Petrich et al., 2012). SNR and dynamic range performance under dim and dynamic light conditions are also key considerations that could potentially be limiting the technology.

Application limits of the technology need therefore to be thoroughly investigated. These include delimiting light levels where the technology is not applicable and other environmental or logistical deployment constraints impeding target detection, underwater georeferencing and image composition (Dumke et al., 2018). For example, image composition and quality might be limited for a scanning pushbroom sensor under a turbulent underwater regimes (Figure 5). In addition, as HI can be expensive and prohibitive, we need to work towards identifying the most cost-effective solutions for each specific situation and target (e.g., testing band specific imaging cameras). Simulation sea-ice tanks with controlled algae cultures and light levels will be useful platforms for further testing of key parameters for the development of this methodology (Cimoli et al., 2017a).

From a data processing perspective, the amount of HI data can be overwhelming and is not straightforward to identify relevant information with such a vast array of data. Multivariate and other statistical approaches have led to several powerful tools in support of hyperspectral remote sensing data analysis (Amigo et al., 2015; Chang and Chang, 2013). However, there are fundamental differences between applications of the technology in typical, above surface, remote sensing applications. Hyperspectral frames from hypothetical upward looking under-ice sensors would acquire images in transmission mode rather than reflection mode, and there are challenges associated with transmission HI compared to reflected light HI which would need to be considered and further investigated for an *in situ* application (Cimoli et al., 2017a).

4.5 Water column correction and immersion effect

In marine optical remote sensing, the water column can have a considerable impact in the traversing electromagnetic radiation depending on its composition and presence of optically active elements such as

phytoplankton, suspended particles and CDOM (Morel and Maritorena, 2001). Except for some cases of very high and concentrated algal blooms below the ice (Arrigo et al., 2012), polar under-ice waters are generally characterised by low concentrations of biomass in the water column compared to those observed in the ice (albeit this is depending on the season and region) (Arrigo et al., 2014; Gradinger, 2009; Spindler, 1994). Assuming no phytoplankton blooms, for sensors deployed near the ice sub-surface, the effect of the water column can be considered negligible at low distances < 0.5 m (Campbell et al., 2015; Melbourne-Thomas et al., 2015). However, increasing the distance between the ice subsurface and the sensor would increase the amount of matter in the optical path and thus disqualifying the previous assumption, e.g., in cases where UUVs are required to be deployed at increased water depth. Increased water depths would result not only in a reduction of light availability and changed spectral properties of the measured light, but could result in the overestimation of biomass in the ice due to the interference of phytoplankton and thus chl-*a* in the overlying water column (Figure 5). Overall, it is not possible to define locations or periods of the year where the water column effect could be considered negligible, and this should be verified at every survey when possible.

To correct for water-column effects, the most straightforward method is to estimate the water column spectral attenuation coefficient K_d (λ) by means of irradiance profiles (Morel and Maritorena, 2001). This yields the extinction characteristics of the local seawater and can be applied to the optical data collected at depth by UUVs (Nicolaus and Katlein, 2013).

If larger distances are to be covered (e.g., through UUVs), it is important to account for any variability of the water column optical properties under-ice (Frey et al., 2011). Spatial variability in water column optical properties could be assessed by performing multiple vertical irradiance profiles to assess spatial variability of such properties.

For hypothetical long-range UUVs transects, water column correction methods would open a challenging research front involving the acquisition of optical properties of the water column simultaneously with the hyperspectral data collection. Measured absorption and scattering properties can then be input into radiative transfer equations to calculate the influence of the water column over the composed imagery (Johnsen et al., 2013). Nevertheless, methods usually applied in marine remote sensing such as modeling of the water column trough radiative transfer will remain challenging in under-ice waters due to the high horizontal variations in structure producing highly variable under-ice light fields (Katlein et al., 2015a).

In case of small-scale HI of the ice-water interface, water column effects can be corrected using standard techniques such as the empirical line method with known reflectance targets (Chennu et al., 2013; Smith and Milton, 1999) or through localized, depth-integrated, irradiance measurements and estimations of inherent and apparent optical properties (Johnsen et al., 2013).

Finally, for radiometers or hyperspectral imagers alike to be immersed in water, specifically designed enclosures are required to safeguard the instrument integrity and efficiency (Zibordi, 2006). Usually, calibration files are provided for off-the-shelf sensors that are designed for underwater deployment. However, HI cameras or other desirable radiometric instruments that have not been designed for in water use would require customized sealed enclosures. These enclosures can introduce spectral and geometrical aberrations whose description is out of the scope of this review. Due to the significant influence on any optical calibrations, and compounding uncertainties associated with different lens materials and geometries, it suffices to say that calibration might be necessary for any additional medium between the sensor and the target under investigation. Particularly if high accuracy radiometric and geometric data are required (Zibordi and Voss, 2014).

5 Outlook for future research opportunities

This review briefly summarized the primary environmental drivers of ice algal biomass spatial variability (Figure 2) and the efforts towards its quantification over multiple spatial scales (Table 1). Observational studies generally comprise only single-year observations of limited areal coverage from one locality and data series often cover a very limited time frame, e.g., scattered days, and weeks to months (Table 1). This hinders quantitative variability estimates and the separation of spatial from temporal variability with consequences for the understanding of seasonal and inter-annual trends (Leu et al., 2015).

One of the greatest advantages of the reviewed close-range remote sensing techniques is that they are non-invasive. This allows for change detection studies of biomass abundance together with other sea-ice properties such as snow depth, ice thickness, nutrients and salinity to be made over time whilst the sea ice persists in single locations. A first temporal (weekly) non-invasive survey of biomass variability has been conducted on Arctic fast ice (Campbell et al., 2015, 2014). Future studies should aim to capture the full annual cycle in sea ice algal dynamics and should target different sea-ice types and regions (Meiners et al., 2017; Leu et al., 2015; Vancoppenolle et al., 2013). The temporal coverage of the time series analyses could eventually be extended over longer periods of time through modern set-up stations of simultaneous, autonomous and high temporal resolution transmittance measurements (Nicolaus et al., 2010).

A second advantage of the methodology is that sensors can be installed on UUVs, thus paving the way to sea-ice biomass mapping at unprecedented spatial resolutions over the mesoscale (e.g., Meiners et al., 2017). Several survey types could be designed from L-shape transects to

hierarchical approaches or entire 2-dimensional areal coverages. This would further permit application of improved geostatistical analyses such as variograms (Oliver and Webster, 2014), which would help to identify, quantify and parametrize key environmental drivers of ice algal biomass (Meiners et al., 2017; Katlein et al., 2015a). Higher spatial coverage and sampling frequencies of the surveys would also permit a better assessment of environmental controls by employing statistical tools like analysis of variance (ANOVA) (Steffens et al., 2006) or spatial autocorrelation (Rysgaard et al., 2001) previously employed through ice coring surveys. In this context, spatial biomass estimates could be coupled with other state-of-the-art methods to determine 3-dimensional floe-scale sea-ice physical properties such as ice thickness (Williams et al., 2014), under-ice topography (Lucieer et al., 2016) or snow depth (Cimoli et al., 2017b).

In comparison to standard point sampling radiometers, HI would allow the extension of such surveys in a spatially continuous dimension which is extremely relevant if we consider the high variability of both ice algal biomass and sea-ice physical properties at multiple spatial scales. HI deployed at specific distances from the ice-water interface might allow monitoring algae distribution at any targeted spatial scale. For example, coupling under-ice HI with rugosity parameters, as a measure of surface roughness, might increase our understanding of algal aggregation and distribution similar to existing coral or benthic mapping studies (e.g., Dustan et al., 2013; Friedman et al., 2012). In addition, standard upward looking RGB cameras as additional payloads not only could help to confirm the status of under-ice physical environment and assisting in the interpretation of data (Fritsen et al., 2011), but could also provide further information for assessing grazer presence and quantitative roughness coefficients (Irvine-Fynn et al., 2014).

Finally, while this review focusses on biomass estimates, novel studies are outlining the potential to combine measurements of *in-vitro* photosynthetic parameters with under-ice remotely sensed estimates of chl-*a*, thereby presenting interesting research prospects to estimate ice algal production (Lange et al., 2017b).

Acknowledgments This research was supported by the Australian Research Council's Special Research Initiative for Antarctic Gateway Partnership (Project ID SR140300001). EC was supported by the Antarctic Gateway Partnership and the University of Tasmania's Institute for Marine and Ph.D. program. KMMs contribution to this work was supported by the Australian Governments Cooperative Research Centres Program through the Antarctic Climate and Ecosystems Cooperative Research Centre, through Australian Antarctic Science project #4298 and through a fellowship at the Hanse-Wissenschaftskolleg (Delmenhorst, Germany). LCLH's contribution to the work was supported by AUFF (Aarhus University Research Foundation) grant nr. 20858. (Delmenhorst, Germany). LCLH's contribution to the work was supported by AUFF (Aarhus University Research Foundation) grant nr. 20858. Our thanks go to the international panel of four anonymous reviewers for their thorough constructive reviews.

References

Adão T, Hruška J, Pádua L, et al. 2017. Hyperspectral imaging: A review on UAV-based sensors, data processing and applications for agriculture and forestry. Remote Sens, 9(11): 1110, doi: 10.3390/rs9111110

Alou-Font E, Mundy C J, Roy S, et al. 2013. Snow cover affects ice algal pigment composition in the coastal Arctic Ocean during spring. Mar Ecol Prog Ser, 474: 89–104, doi: 10.3354/meps10107

Ambrose Jr W G, Von Quillfeldt C, Clough L M, et al. 2005. The sub-ice algal community in the Chukchi Sea: Large- and small-scale patterns of abundance based on images from a remotely operated vehicle. Polar Biol, 28(10): 784–795, doi: 10.1007/s00300-005-0002-8

Amigo J M, Babamoradi H, Elcoroaristizabal S. 2015. Hyperspectral image analysis. a tutorial. Anal Chim Acta, 896: 34–51, doi: 10.1016/j.aca.2015.09.030

Arndt S, Meiners K M, Ricker R, et al. 2017. Influence of snow depth and surface flooding on light transmission through Antarctic pack ice. J Geophys Res, 122(3): 2108–2119, doi: 10.1002/2016JC012325

Arrigo K R. 2017. Sea ice as a habitat for primary producers// Thomas D N. Sea ice. 3rd edn. Washington, D.C.: John Wiley & Sons, Ltd, 352–369, doi: 10.1002/9781118778371.ch14

Arrigo K R. 2014. Sea ice ecosystems. Ann Rev Mar Sci, 6: 439–467, doi: 10.1146/annurev-marine-010213-135103

Arrigo K R, Brown Z W, Mills M M. 2014. Sea ice algal biomass and physiology in the Amundsen Sea, Antarctica. Elem Sci Anth, 2: 000028, doi: 10.12952/journal.elementa.000028

Arrigo K R, Dieckmann G, Gosselin M, et al. 1995. High resolution study of the platelet ice ecosystem in McMurdo Sound, Antarctica: biomass, nutrient, and production profiles within a dense microalgal bloom. Mar Ecol Prog Ser, 127: 255–268, doi: 10.3354/meps127255

Arrigo K R, Mock T, Lizotte M P. 2010. Primary producers and sea ice//Thomas D N, Dieckmann G S. Sea ice. 2nd edn. Washington, D.C.: Wiley-Blackwell, 283–325

Arrigo K R, Perovich D K, Pickart R S, et al. 2012. Massive phytoplankton blooms under arctic sea ice. Science, 336(6087): 1408, doi: 10.1126/science.1215065

Arrigo K R, Sullivan C W, Kremer J N. 1991. A bio-optical model of Antarctic sea ice. J Geophys Res, 96(C6): 10581–10592

Bioucas-Dias J M, Plaza A, Camps-Valls G, et al. 2013. Hyperspectral remote sensing data analysis and future challenges. IEEE Geosci Remote Sens Mag, 1(2): 6–36, doi: 10.1109/MGRS.2013.2244672

Blackburn G A. 2007. Hyperspectral remote sensing of plant pigments. J Exp Bot, 58(4): 855–867, doi: 10.1093/jxb/erl123

Bluhm B A, Swadling K M, Gradinger R. 2017. Sea ice as a habitat for macrograzers//Thomas D N. Sea ice. 3rd edn.

Washington, D.C.: John Wiley & Sons, Ltd, 394–414, doi: 10.1002/9781118778371.ch16

Boetius A, Albrecht S, Bakker K, et al. 2013. Export of algal biomass from the melting Arctic sea ice. Science, 339(6126): 1430–1432, doi: 10.1126/science.1231346

Buchhorn M, Raynolds M K, Walker D A. 2016. Influence of BRDF on NDVI and biomass estimations of Alaska Arctic tundra. Environ Res Lett, 11(12): 125002, doi: 10.1088/1748-9326/11/12/125002

Campbell K, Mundy C J, Barber D G, et al. 2015. Characterizing the sea ice algae chlorophyll a–snow depth relationship over Arctic spring melt using transmitted irradiance. J Mar Syst, 147: 76–84, doi: 10.1016/j.jmarsys.2014.01.008

Campbell K, Mundy C J, Barber D G, et al. 2014. Remote estimates of ice algae biomass and their response to environmental conditions during spring melt. Arctic, 67(3): 375–387, doi: 10.14430/arctic4409

Castellani G, Losch M, Lange B A, et al. 2017. Modeling arctic sea ice algae: Physical drivers of spatial distribution and algae phenology. J Geophys Res, 122(9): 7466–7487, doi: 10.1002/2017JC012828

Chang C I. 2013. Hyperspectral data processing: algorithm design and analysis. Hoboken, NJ: John Wiley & Sons, Inc.

Chennu A, Färber P, De'ath G, et al. 2017. A diver-operated hyperspectral imaging and topographic surveying system for automated mapping of benthic habitats. Sci Rep, 7: 7122, doi: 10.1038/s41598-017-07337-y

Chennu A, Färber P, Volkenborn N, et al. 2013. Hyperspectral imaging of the microscale distribution and dynamics of microphytobenthos in intertidal sediments. Limnol Oceanogr, 11(10): 511–528, doi: 10.4319/lom.2013.11.511

Cimoli E, Lucieer A, Meiners K M, et al. 2017a. Towards improved estimates of sea ice algal biomass: experimental assessment of hyperspectral imaging cameras for under-ice studies. Ann Glaciol, 58(75pt1): 68–77, doi: 10.1017/aog.2017.6

Cimoli E, Marcer M, Vandecrux B, et al. 2017b. Application of low-cost UASs and digital photogrammetry for high-resolution snow depth mapping in the Arctic. Remote Sens, 9(11): 1144, doi: 10.3390/rs9111144

Cota G F, Smith R E H. 1991. Ecology of bottom ice algae: II. Dynamics, distributions and productivity. J Mar Syst, 2(3–4): 279–295, doi: 10.1016/0924-7963(91)90037-U

Cox G F N, Weeks W F. 1983. Equations for determining the gas and brine volumes in sea ice samples. J Glaciol, 29(102): 306–316

Dumke I, Nornes S M, Purser A, et al. 2018. First hyperspectral imaging survey of the deep seafloor: High-resolution mapping of manganese nodules. Remote Sens Environ, 209: 19–30, doi: 10.1016/j.rse.2018.02.024

Dustan P, Doherty O, Pardede S. 2013. Digital reef rugosity estimates coral reef habitat complexity. PLoS One, 8(2): e57386, doi: 10.1371/journal.pone.0057386

Edelman G J, Gaston E, Van Leeuwen T G, et al. 2012. Hyperspectral imaging for non-contact analysis of forensic traces. Forensic Sci Int, 223(1–3): 28–39, doi: 10.1016/j.forsciint.2012.09.012

Ehn J K, Mundy C J. 2013. Assessment of light absorption within highly scattering bottom sea ice from under-ice light measurements: implications for Arctic ice algae primary production. Limnol Oceanogr, 58(3): 893–902

Eicken H, Lange M A, Dieckmann G S. 1991. Spatial variability of sea ice properties in the northwestern Weddell Sea. J Geophys Res, 96(C6): 10603–10615, doi: 10.1029/91JC00456

Fiala M, Kuosa H, Kopczyńska E E, et al. 2006. Spatial and seasonal heterogeneity of sea ice microbial communities in the first-year ice of Terre Adélie area (Antarctica). Aquat Microb Ecol, 43(1): 95–106

Flores H, Atkinson A, Kawaguchi S, et al. 2012. Impact of climate change on Antarctic krill. Mar Ecol Prog Ser, 458: 1–19, doi: 10.3354/meps09831

Forrest A L, Lund-Hansen L C, Sorrell B K, et al. 2016. Brief communication: Capturing scales of spatial heterogeneity of Antarctic sea ice algae communities. Cryosphere Discuss, doi: 10.5194/tc-2016-186

Frey K E, Perovich D K, Light B. 2011. The spatial distribution of solar radiation under a melting Arctic sea ice cover. Geophys Res Lett, 38(22): L22501, doi: 10.1029/2011GL049421

Friedman A, Pizarro O, Williams S B, et al. 2012. Multi-scale measures of rugosity, slope and aspect from benthic stereo image reconstructions. PLoS One, 7(12): e50440, doi: 10.1371/journal.pone.0050440

Fritsen C H, Iturriaga R H, Sullivan C W. 1992. Influence of particulate matter on spectral irradiance fields and energy transfer in the Eastern Arctic Ocean//Proceedings Volume 1750, Ocean Optics XI. San Diego, CA: SPIE, 527–541, doi: 10.1117/12.140679

Fritsen C H, Wirthlin E D, Momberg D K, et al. 2011. Bio-optical properties of Antarctic pack ice in the early austral spring. Deep Sea Res Part II Top Stud Oceanogr, 58(9–10): 1052–1061, doi: 10.1016/j.dsr2.2010.10.028

Galindo V, Gosselin M, Lavaud J, et al. 2017. Pigment composition and photoprotection of Arctic sea ice algae during spring. Mar Ecol Prog Ser, 585: 49–69, doi: 10.3354/meps12398

Garrison D L, Buck K B. 1991. Surface-layer sea ice assemblages in Antarctic pack ice during the austral spring: environmental conditions, primary production and community structure. Mar Ecol Prog Ser, 75(2): 161–172

Gosselin M, Legendre L, Therriault J C, et al. 1986. Physical control of the horizontal patchiness of sea ice microalgae. Mar Ecol Prog Ser, 29: 289–298

Gradinger R. 2009. Sea ice algae: Major contributors to primary production and algal biomass in the Chukchi and Beaufort Seas during May/June 2002. Deep Sea Res Part II Top Stud Oceanogr, 56(17): 1201–1212, doi: 10.1016/j.dsr2.2008.10.016

Gradinger R, Ikävalko J. 1998. Organism incorporation into newly forming Arctic sea ice in the Greenland Sea. J Plankton Res, 20(5): 871–886

Gradinger R R, Bluhm B A. 2004. In-situ observations on the distribution and behavior of amphipods and Arctic cod (Boreogadus saida) under the sea ice of the High Arctic Canada Basin. Polar Biol, 27(10): 595–603, doi: 10.1007/s00300-004-0630-4

Granskog M A, Kaartokallio H, Kuosa H, et al. 2005. Scales of horizontal patchiness in chlorophyll a, chemical and physical

properties of landfast sea ice in the Gulf of Finland (Baltic Sea). Polar Biol, 28(4): 276–283, doi: 10.1007/s00300-004-0690-5

Gutt J. 1995. The occurrence of sub-ice algal aggregations off northeast Greenland. Polar Biol, 15(4): 247–252, doi: 10.1007/BF00239844

Hamre B, Winther J G, Gerland S, et al. 2004. Modeled and measured optical transmittance of snow-covered first-year sea ice in Kongsfjorden, Svalbard. J Geophys Res, 109(C10): C10006, doi: 10.1029/2003JC001926

Hancke K, Lund-Hansen L C, Lamare M L, et al. 2018. Extreme low light requirement for algae growth underneath sea ice: A case study from station Nord, NE Greenland. J Geophys Res, 123(2): 985–1000, doi: 10.1002/2017JC013263

Hawes I, Lund-Hansen L C, Sorrell B K, et al. 2012. Photobiology of sea ice algae during initial spring growth in Kangerlussuaq, West Greenland: Insights from imaging variable chlorophyll fluorescence of ice cores. Photosynth Res, 112(2): 103–115, doi: 10.1007/s11120-012-9736-7

Holm-Hansen O, Riemann B. 1978. Chlorophyll a determination: improvements in methodology. Oikos, 30(3): 438–447, doi: 10.2307/3543338

Horner R, Ackley S F, Dieckmann G S, et al. 1992. Ecology of sea ice biota: 1. Habitat, terminology, and methodology. Polar Biol, 12(3–4): 417–427

Huang H, Liu L, Ngadi M O. 2014. Recent developments in hyperspectral imaging for assessment of food quality and safety. Sensors, 14(4): 7248–7276, doi: 10.3390/s140407248

Irvine-Fynn T D L, Sanz-Ablanedo E, Rutter N, et al. 2014. Measuring glacier surface roughness using plot-scale, close-range digital photogrammetry. J Glaciol, 60(223): 957–969, doi: 10.3189/2014JoG14J032

Janssens J, Meiners K M, Tison J L, et al. 2016. Incorporation of iron and organic matter into young Antarctic sea ice during its initial growth stages. Elem Sci Anth, 4(1): 000123, doi: 10.12952/journal.elementa.000123

Johnsen G, Hegseth E N. 1991. Photoadaptation of sea ice microalgae in the Barents Sea. Polar Biol, 11(3): 179–184

Johnsen G, Sakshaug E. 2007. Biooptical characteristics of PSII and PSI in 33 species (13 pigment groups) of marine phytoplankton, and the relevance for pulse-amplitude-modulated and fast-repetition-rate fluorometry. J Phycol, 43(6): 1236–1251, doi: 10.1111/j.1529-8817.2007.00422.x

Johnsen G, Volent Z, Dierssen H, et al. 2013. Underwater hyperspectral imagery to create biogeochemical maps of seafloor properties//Watson J E, Zielinski O. Subsea optics and imaging. Cambridge: Woodhead Publishing, 508–540e

Juhl A R, Krembs C. 2010. Effects of snow removal and algal photoacclimation on growth and export of ice algae. Polar Biol, 33(8): 1057–1065, doi: 10.1007/s00300-010-0784-1

Kaartokallio H, Granskog M A, Kuosa H, et al. 2017. Ice in subarctic seas//Thomas D N. Sea ice. 3rd edn. Washington, D.C.: John Wiley & Sons, Ltd, 630–644, doi: 10.1002/9781118778371.ch27

Katlein C, Arndt S, Nicolaus M, et al. 2015a. Influence of ice thickness and surface properties on light transmission through Arctic sea ice. J Geophys Res, 120(9): 5932–5944, doi: 10.1002/2015JC010914

Katlein C, Fernández-Méndez M, Wenzhöfer F, et al. 2015b. Distribution of algal aggregates under summer sea ice in the Central Arctic. Polar Biol, 38(5): 719–731, doi: 10.1007/s00300-014-1634-3

Katlein C, Nicolaus M, Petrich C. 2014. The anisotropic scattering coefficient of sea ice. J Geophys Res, 119(2): 842–855, doi: 10.1002/2013JC009502

Katlein C, Perovich D K, Nicolaus M. 2016. Geometric effects of an inhomogeneous sea ice cover on the under ice light field. Front Earth Sci, 4: 6

Kattner G, Thomas D N, Haas C, et al. 2004. Surface ice and gap layers in Antarctic sea ice: Highly productive habitats. Mar Ecol Prog Ser, 277: 1–12, doi: 10.3354/meps277001

Kauko H M, Taskjelle T, Assmy P, et al. 2017. Windows in arctic sea ice: light transmission and ice algae in a refrozen lead. J Geophys Res, 122(6): 1486–1505, doi: 10.1002/2016JG003626

Kirk J T O. 2011. Light and photosynthesis in aquatic ecosystems. 3rd edn. Cambridge , New York: Cambridge University Press,

Kohlbach D, Graeve M, Lange B A, et al. 2016. The importance of ice algae-produced carbon in the central Arctic Ocean ecosystem: food web relationships revealed by lipid and stable isotope analyses. Limnol Oceanogr, 61(6): 2027–2044, doi: 10.1002/lno.10351

Kohlbach D, Lange B A, Schaafsma F L, et al. 2017. Ice algae-produced carbon is critical for overwintering of Antarctic krill Euphausia Superba. Front Mar Sci, 4: 310, doi: 10.3389/fmars.2017.00310

Krembs C, Gradinger R, Spindler M. 2000. Implications of brine channel geometry and surface area for the interaction of sympagic organisms in Arctic sea ice. J Exp Mar Biol Ecol, 243(1): 55–80, doi: 10.1016/S0022-0981(99)00111-2

Krembs C, Mock T, Gradinger R. 2001. A mesocosm study of physical-biological interactions in artificial sea ice: effects of brine channel surface evolution and brine movement on algal biomass. Polar Biol, 24(5): 356–364, doi: 10.1007/s003000000219

Krembs C, Tuschling K, Juterzenka K V. 2002. The topography of the ice-water interface – its influence on the colonization of sea ice by algae. Polar Biol, 25(2): 106–117, doi: 10.1007/s003000100318

Lange B A, Flores H, Michel C, et al. 2017a. Pan-Arctic sea ice-algal chl a biomass and suitable habitat are largely underestimated for multiyear ice. Glob Change Biol, 23(11): 4581–4597, doi: 10.1111/gcb.13742

Lange B A, Katlein C, Castellani G, et al. 2017b. Characterizing spatial variability of ice algal chlorophyll a and net primary production between sea ice habitats using horizontal profiling platforms. Front Mar Sci, 4: 349, doi: 10.3389/fmars.2017.00349

Lange B A, Katlein C, Nicolaus M, et al. 2016. Sea ice algae chlorophyll *a* concentrations derived from under-ice spectral radiation profiling platforms. J Geophys Res, 121(12): 8511–8534, doi: 10.1002/2016JC011991

Lange B A, Michel C, Beckers J F, et al. 2015. Comparing springtime ice-algal chlorophyll a and physical properties of multi-year and first-year sea ice from the Lincoln sea. PLoS One, 10(4): e0122418, doi: 10.1371/journal.pone.0122418

Langhorne P J, Hughes K G, Gough A J, et al. 2015. Observed platelet ice distributions in Antarctic sea ice: An index for ocean-ice shelf heat flux. Geophys Res Lett, 42(13): 5442–5451, doi: 10.1002/2015GL064508

Legendre L, Gosselin M. 1991. In situ spectroradiometric estimation of microalgal biomass in first-year sea ice. Polar Biol, 11(2): 113–115, doi: 10.1007/BF00234273

Leu E, Mundy C J, Assmy P, et al. 2015. Arctic spring awakening – Steering principles behind the phenology of vernal ice algal blooms. Prog Oceanogr, 139: 151–170, doi: 10.1016/j.pocean.2015.07.012

Li Z J, Li R L, Wang Z P, et al. 2016. Upper limits for chlorophyll *a* changes with brine volume in sea ice during the austral spring in the Weddell Sea, Antarctica. Acta Oceanol Sin, 35(2): 68–75, doi: 10.1007/s13131-015-0740-6

Light B, Maykut G A, Grenfell T C. 2004. A temperature-dependent, structural-optical model of first-year sea ice. J Geophys Res, 109(C6): C06013, doi: 10.1029/2003JC002164

Liu Z Y, Li C J, Wang Y T, et al. 2011. Comparison of spectral indices and principal component analysis for differentiating lodged rice crop from normal ones//Proceedings of the 5th IFIP TC 5/SIG 5.1 Conference on Computer and Computing Technologies in Agriculture. Beijing: Springer, 84–92

Lizotte M P. 2001. The contributions of sea ice algae to Antarctic marine primary production. Am Zool, 41(1): 57–73

Lu G L, Fei B W. 2014. Medical hyperspectral imaging: a review. J Biomed Opt, 19(1): 010901, doi: 10.1117/1.JBO.19.1.010901

Lucieer V, Nau A W, Forrest A L, et al. 2016. Fine-scale sea ice structure characterized using underwater acoustic methods. Remote Sens, 8(10): 821, doi: 10.3390/rs8100821

Ludvigsen M, Johnsen G, Lågstad P A, et al. 2013. Scientific operations combining ROV and AUV in the Trondheim Fjord//Proceedings of 2013 MTS/IEEE OCEANS-Bergen. Bergen: IEEE, 1–7

Lund-Hansen L C, Hawes I, Nielsen M H, et al. 2017. Is colonization of sea ice by diatoms facilitated by increased surface roughness in growing ice crystals? Polar Biol, 40(3): 593–602, doi: 10.1007/s00300-016-1981-3

Lund-Hansen L C, Hawes I, Sorrell B K, et al. 2014. Removal of snow cover inhibits spring growth of Arctic ice algae through physiological and behavioral effects. Polar Biol, 37(4): 471–481, doi: 10.1007/s00300-013-1444-z

Lund-Hansen L C, Juul T, Eskildsen T D, et al. 2018. A low-cost remotely operated vehicle (ROV) with an optical positioning system for under-ice measurements and sampling. Cold Reg Sci Technol, 151: 148–155, doi: 10.1016/j.coldregions.2018.03.017

Lund-Hansen L C, Markager S, Hancke K, et al. 2015. Effects of sea ice light attenuation and CDOM absorption in the water below the Eurasian sector of central Arctic Ocean (>88°N). Polar Res, 34(1): 23978, doi: 10.3402/polar.v34.23978

Maestrini S Y, Rochet M, Legendre L, et al. 1986. Nutrient limitation of the bottom-ice microalgal biomass (southeastern Hudson Bay, Canadian Arctic). Limnol Oceanogr, 31(5): 969–982, doi: 10.4319/lo.1986.31.5.0969

Mäkynen J, Saari H, Holmlund C, et al. 2012. Multi- and hyperspectral UAV imaging system for forest and agriculture applications//Proceedings of Volume 8374, Next-Generation Spectroscopic Technologies V. Baltimore, Maryland: SPIE, 837409, doi: 10.1117/12.918571

Massom R A, Eicken H, Hass C, et al. 2001. Snow on Antarctic sea ice. Rev Geophys, 39(3): 413–445, doi: 10.1029/2000RG000085

Massom R A, Stammerjohn S E. 2010. Antarctic sea ice change and variability – Physical and ecological implications. Polar Sci, 4(2): 149–186, doi: 10.1016/j.polar.2010.05.001

Maykut G A, Grenfell T C. 1975. The spectral distribution of light beneath first-year sea ice in the Arctic Ocean. Limnol Oceanogr, 20(4): 554–563, doi: 10.4319/lo.1975.20.4.0554

Mcdonald S, Koulis T, Ehn J, et al. 2015. A functional regression model for predicting optical depth and estimating attenuation coefficients in sea ice covers near Resolute Passage, Canada. Ann Glaciol, 56(69): 147–154, doi: 10.3189/2015AoG69A004

McMinn A, Ashworth C, Bhagooli R, et al. 2012. Antarctic coastal microalgal primary production and photosynthesis. Mar Biol, 159(12): 2827–2837, doi: 10.1007/s00227-012-2044-0

McMinn A, Hegseth E N. 2007. Sea ice primary productivity in the northern Barents Sea, spring 2004. Polar Biol, 30(3): 289–294, doi: 10.1007/s00300-006-0182-x

McMinn A, Ryan K G, Ralph P J, et al. 2007. Spring sea ice photosynthesis, primary productivity and biomass distribution in eastern Antarctica, 2002–2004. Mar Biol, 151(3): 985–995, doi: 10.1007/s00227-006-0533-8

Mehrubeoglu M, Teng M Y, Zimba P V. 2014. Resolving mixed algal species in hyperspectral images. Sensors, 14(1): 1–21, doi: 10.3390/s140100001

Meiners K M, Arndt S, Bestley S, et al. 2017. Antarctic pack ice algal distribution: Floe-scale spatial variability and predictability from physical parameters. Geophys Res Lett, 44(14): 7382–7390, doi: 10.1002/2017GL074346

Meiners K M, Michel C. 2017. Dynamics of nutrients, dissolved organic matter and exopolymers in sea ice//Thomas D N. Sea ice. 3rd edn. Washington, D.C.: John Wiley & Sons, Inc, 415–432, doi: 10.1002/9781118778371.ch17

Meiners K M, Norman L, Granskog M A, et al. 2011. Physico-ecobiogeochemistry of East Antarctic pack ice during the winter-spring transition. Deep Sea Res Part II Top Stud Oceanogr, 58(9–10): 1172–1181, doi: 10.1016/j.dsr2.2010.10.033

Meiners K M, Vancoppenolle M, Thanassekos S, et al. 2012. Chlorophyll a in Antarctic sea ice from historical ice core data. Geophys Res Lett, 39(21): L21602, doi: 10.1029/2012GL053478

Melbourne-Thomas J, Meiners K M, Mundy C J, et al. 2015. Algorithms to estimate Antarctic sea ice algal biomass from under-ice irradiance spectra at regional scales. Mar Ecol Prog Ser, 536: 107–121

Michel C, Nielsen T G, Nozais C, et al. 2002. Significance of sedimentation and grazing by ice micro- and meiofauna for carbon cycling in annual sea ice (northern Baffin Bay). Aquat Microb Ecol, 30: 57–68, doi: 10.3354/ame030057

Miller L A, Fripiat F, Else B G T, et al. 2015. Methods for biogeochemical studies of sea ice: the state of the art, caveats, and recommendations. Elem Sci Anth, 3: 000038, doi:

10.12952/journal.elementa.000038
Moberg L, Karlberg B, Sørensen K, et al. 2002. Assessment of phytoplankton class abundance using absorption spectra and chemometrics. Talanta, 56(1): 153–160
Moisan J R, Moisan T A H, H Linkswiler M A. 2011. An inverse modeling approach to estimating phytoplankton pigment concentrations from phytoplankton absorption spectra. J Geophys Res, 116(C9): C09018, doi: 10.1029/2010JC006786
Monti D, Legendre L, Therriault J C, et al. 1996. Horizontal distribution of sea ice microalgae: environmental control and spatial processes (southeastern Hudson Bay, Canada). Mar Ecol Prog Ser, 133: 229–240
Morel A, Bricaud A. 1981. Theoretical results concerning light absorption in a discrete medium, and application to specific absorption of phytoplankton. Deep Sea Res Part A Oceanogr Res Pap, 28(11):1375–1393
Morel A, Maritorena S. 2001. Bio-optical properties of oceanic waters: a reappraisal. J Geophys Res, 106(C4): 7163–7180
Mundy C J, Barber D G, Michel C. 2005. Variability of snow and ice thermal, physical and optical properties pertinent to sea ice algae biomass during spring. J Mar Syst, 58(3–4): 107–120, doi: 10.1016/j.jmarsys.2005.07.003
Mundy C J, Ehn J K, Barber D G, et al. 2007. Influence of snow cover and algae on the spectral dependence of transmitted irradiance through Arctic landfast first-year sea ice. J Geophys Res, 112(C3): C03007, doi: 10.1029/2006JC003683
Mundy C J, Gosselin M, Gratton Y, et al. 2014. Role of environmental factors on phytoplankton bloom initiation under landfast sea ice in Resolute Passage, Canada. Mar Ecol Prog Ser, 497: 39–49, doi: 10.3354/meps10587
Nicolaus M, Hudson S R, Gerland S, et al. 2010. A modern concept for autonomous and continuous measurements of spectral albedo and transmittance of sea ice. Cold Reg Sci Technol, 62(1): 14–28, doi: 10.1016/j.coldregions.2010.03.001
Nicolaus M, Katlein C. 2013. Mapping radiation transfer through sea ice using a remotely operated vehicle (ROV). Cryosphere, 7(3): 763–777, doi: 10.5194/tc-7-763-2013
Nicolaus M, Petrich C, Hudson S R, et al. 2013. Variability of light transmission through Arctic land-fast sea ice during spring. Cryosphere, 7(3): 977–986, doi: 10.5194/tc-7-977-2013
Norgren P, Skjetne R. 2014. Using autonomous underwater vehicles as sensor platforms for ice-monitoring. Model Identif Control, 35(4): 263–277, doi: 10.4173/mic.2014.4.4
Norman L, Thomas D N, Stedmon C A, et al. 2011. The characteristics of dissolved organic matter (DOM) and chromophoric dissolved organic matter (CDOM) in Antarctic sea ice. Deep Sea Res Part II Top Stud Oceanogr, 58(9–10): 1075–1091
Oliver M A, Webster R. 2014. A tutorial guide to geostatistics: Computing and modelling variograms and kriging. CATENA, 113: 56–69, doi: 10.1016/j.catena.2013.09.006
Olsen L M, Laney S R, Duarte P, et al. 2017. The seeding of ice algal blooms in Arctic pack ice: the multiyear ice seed repository hypothesis. J Geophys Res, 122(7): 1529–1548, doi: 10.1002/2016JG003668
Palmer J M, Grant B G. 2010. The art of radiometry. Bellingham: SPIE Press
Palmisano A C, Soohoo J B, Moe R L, et al. 1987. Sea ice microbial communities. VII. Changes in under-ice spectral irradiance during the development of Antarctic sea ice microalgal communities. Mar Ecol Prog Ser, 35: 165–173
Perkins R G, Williamson C J, Brodie J, et al. 2016. Microspatial variability in community structure and photophysiology of calcified macroalgal microbiomes revealed by coupling of hyperspectral and high-resolution fluorescence imaging. Sci Rep, 6: 22343, doi: 10.1038/srep22343
Perovich D K. 2017. Sea ice and sunlight//Thomas D N. Sea ice. 3rd edn. Washington, D.C.: John Wiley & Sons, Inc., 110–137, doi: 10.1002/9781118778371.ch4
Perovich D K. 2007. Light reflection and transmission by a temperate snow cover. J Glaciol, 53(181): 201–210
Perovich D K. 1996. The optical properties of sea ice. US Army Corps of Engineers: 24
Perovich D K. 1989. A two-stream multilayer, spectral radiative transfer model for sea ice. Defense Technical Information Center (DTIC) Document, USA
Petrich C, Eicken H. 2016. Overview of sea ice growth and properties//Thomas D N. Sea ice. 3rd edn. Chichester: John Wiley & Sons, Ltd, 1–41, doi: 10.1002/9781118778371.ch1
Petrich C, Eicken H. 2009. Growth, structure and properties of sea ice//Thomas D N, Dieckmann G S. Sea ice. 2nd edn. Oxford: Wiley-Blackwell, 23–77
Petrich C, Nicolaus M, Gradinger R. 2012. Sensitivity of the light field under sea ice to spatially inhomogeneous optical properties and incident light assessed with three-dimensional Monte Carlo radiative transfer simulations. Cold Reg Sci Technol, 73: 1–11, doi: 10.1016/j.coldregions.2011.12.004
Post E, Bhatt U S, Bitz C M, et al. 2013. Ecological consequences of sea ice decline. Science, 341(6145): 519–524, doi: 10.1126/science.1235225
Raymond B, Meiners K, Fowler C W, et al. 2009. Cumulative solar irradiance and potential large-scale sea ice algae distribution off East Antarctica (30°E–150°E). Polar Biol, 32(3): 443–452, doi: 10.1007/s00300-008-0538-5
Robineau B, Legendre L, Kishino M, et al. 1997. Horizontal heterogeneity of microalgal biomass in the first-year sea ice of Saroma-ko Lagoon (Hokkaido, Japan). J Mar Syst, 11(1–2): 81–91, doi: 10.1016/S0924-7963(96)00030-9
Ryan K G, Hegseth E N, Martin A, et al. 2006. Comparison of the microalgal community within fast ice at two sites along the Ross Sea coast, Antarctica. Antarct Sci, 18(4): 583–594, doi: 10.1017/S0954102006000629
Rysgaard S, Kühl M, Glud R N, et al. 2001. Biomass, production and horizontal patchiness of sea ice algae in a high-Arctic fjord (Young Sound, NE Greenland). Mar Ecol Prog Ser, 223: 15–26
Sibert V, Zakardjian B, Saucier F, et al. 2010. Spatial and temporal variability of ice algal production in a 3D ice-ocean model of the Hudson Bay, Hudson Strait and Foxe Basin system. Polar Res, 29(3): 353–378, doi: 10.1111/j.1751-8369.2010.00184.x
Singh H, Maksym T, Wilkinson J, et al. 2017. Inexpensive, small AUVs for studying ice-covered polar environments. Sci Rob, 2(7): eaan4809 Smith G M, Milton E J. 1999. The use of the empirical line method to calibrate remotely sensed data to reflectance. Int J Remote Sens, 20(13): 2653–2662, doi:

10.1080/014311699211994

Smith W O, Nelson D M. 1985. Phytoplankton bloom produced by a receding ice edge in the ross sea: spatial coherence with the density field. Science, 227(4683): 163–166, doi: 10.1126/science.227.4683.163

SooHoo J B, Palmisano A C, Kottmeier S T, et al. 1987. Spectral light absorption and quantum yield of photosynthesis in sea ice microalgae and a bloom of *Phaeocystis pouchetii* from McMurdo Sound, Antarctica. Mar Ecol Prog Ser, 39: 175–189

Søreide J E, Leu E, Berge J, et al. 2010. Timing of blooms, algal food quality and *Calanus glacialis* reproduction and growth in a changing Arctic. Glob Change Biol, 16(11): 3154–3163, doi: 10.1111/j.1365-2486.2010.02175.x

Spindler M, Dieckmann G S. 1986. Distribution and abundance of the planktic foraminifer *Neogloboquadrina pachyderma* in sea ice of the Weddell Sea (Antarctica). Polar Biol, 5(3): 185–191, doi: 10.1007/BF00441699

Spindler M. 1994. Notes on the biology of sea ice in the Arctic and Antarctic. Polar Biol, 14(5): 319–324

Spindler M. 1990. A comparison of arctic and antarctic sea ice and the effects of different properties on sea ice biota//Bleil U, Thiede J. Geological history of the polar oceans: arctic versus antarctic. NATO ASI Series. Dordrecht: Springer, 173–186, doi: 10.1007/978-94-009-2029-3_10

Steffens M, Granskog M A, Kaartokallio H, et al. 2006. Spatial variation of biogeochemical properties of landfast sea ice in the Gulf of Bothnia, Baltic Sea. Ann Glaciol, 44: 80–87

Steiner N, Deal C, Lannuzel D, et al. 2016. What sea ice biogeochemical modellers need from observers. Elem Sci Anth, 4: 000084, doi: 10.12952/journal.elementa.000084

Swadling K M, Gibson J A E, Ritz D A, et al. 1997. Horizontal patchiness in sympagic organisms of the Antarctic fast ice. Antarct Sci, 9(4): 399–406, doi: 10.1017/S0954102097000515

Tedesco L, Vichi M. 2014. Sea ice biogeochemistry: A guide for modellers. PLoS One, 9(2): e89217

Thomas D N, Dieckmann G S. 2002. Antarctic sea ice–a habitat for extremophiles. Science, 295(5555): 641–644

Tucker W B, Gow A J, Richter J A. 1984. On small-scale horizontal variations of salinity in first-year sea ice. J Geophys Res, 89(C4): 6505–6514

Van Leeuwe M, Tedesco L, Arrigo K R, et al. 2018. Microalgal community structure and primary production in Arctic and Antarctic sea ice: A synthesis. Elem Sci Anth, 6(1): 4, doi: 10.1525/elementa.267

Vancoppenolle M, Meiners K M, Michel C, et al. 2013. Role of sea ice in global biogeochemical cycles: Emerging views and challenges. Quat Sci Rev, 79: 207–230

Wadhams P, Lange M A, Ackley S F. 1987. The ice thickness distribution across the Atlantic sector of the Antarctic Ocean in midwinter. J Geophys Res, 92(C13): 14535–14552, doi: 10.1029/JC092iC13p14535

Wang L A, Zhou X D, Zhu X K, et al. 2016. Estimation of biomass in wheat using random forest regression algorithm and remote sensing data. Crop J, 4(3): 212–219, doi: 10.1016/j.cj.2016.01.008

Warren S G. 1982. Optical properties of snow. Rev Geophys, 20(1): 67–89

Welch H E, Bergmann M A. 1989. Seasonal development of ice algae and its prediction from environmental factors near resolute, N.W.T., Canada. Can J Fish Aquat Sci, 46(10): 1793–1804

Werner I. 1997. Grazing of Arctic under-ice amphipods on sea ice algae. Mar Ecol Prog Ser, 160: 93–99, doi: 10.3354/meps160093

Williams G, Maksym T, Wilkinson J, et al. 2015. Thick and deformed Antarctic sea ice mapped with autonomous underwater vehicles. Nat Geosci, 8: 61–67, doi: 10.1038/ngeo2299

Wongpan P, Meiners K M, Langhorne P J, et al. 2018. Estimation of antarctic land-fast sea ice algal biomass and snow thickness from under-ice radiance spectra in two contrasting areas. J Geophys Res, 123(3): 1907–1923, doi: 10.1002/2017JC013711

Worby A P, Massom R A, Allison I, et al. 1998. East Antarctic sea ice: A review of its structure, properties and drift//Jeffries M O. Antarctic sea ice: physical processes, interactions and variability. Washington: American Geophysical Union, 41–67, doi: 10.1029/AR074p0041

Wynn R B, Huvenne V A I, Le Bas T P, et al. 2014. Autonomous Underwater Vehicles (AUVs): Their past, present and future contributions to the advancement of marine geoscience. Mar Geol, 352: 451–468

Xie H X, Aubry C, Zhang Y, et al. 2014. Chromophoric dissolved organic matter (CDOM) in first-year sea ice in the western Canadian Arctic. Mar Chem, 165: 25–35, doi: 10.1016/j.marchem.2014.07.007

Zeebe R E, Eicken H, Robinson D H, et al. 1996. Modeling the heating and melting of sea ice through light absorption by microalgae. J Geophys Res, 101(C1): 1163–1181

Zhang X D, Huot Y, Bricaud A, et al. 2015. Inversion of spectral absorption coefficients to infer phytoplankton size classes, chlorophyll concentration, and detrital matter. Appl Opt, 54(18): 5805–5816, doi: 10.1364/AO.54.005805

Zibordi G. 2006. Immersion factor of in-water radiance sensors: Assessment for a class of radiometers. J Atmos Ocean Technol, 23(2): 302–313

Zibordi G, Voss K J. 2014. Chapter 3.1 - in situ optical radiometry in the visible and near infrared. Exp Methods Phys Sci, 47: 247–304, doi: 10.1016/B978-0-12-417011-7.00010-6